

UNIVERSITY OF EDUCATION, WINNEBA
COLLEGE OF TECHNOLOGY EDUCATION, KUMASI

DESIGN AND ANALYSIS OF BROADBAND PLANAR SLOT ANTENNA
DESIGN FOR FUTURE COMMUNICATION NETWORKS

BY

DAMBA, ALHASSAN

(200029522)



**A Thesis Submitted to the Department of Electrical/Electronic Engineering,
University of Education, Winneba, In Partial Fulfilment of the Requirements for
the Award of the Degree of Master of Philosophy in Electrical/Electronic
Engineering**

JANUARY, 2022

DECLARATION

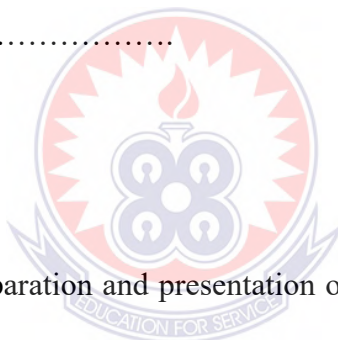
Student's Declaration

I, **DAMBA, ALHASSAN**, declare that this thesis, with the exception of quotations and references contained in published works which have all been identified and duly acknowledged, is entirely my own original work, and it has not been submitted, either in part or whole, for another degree elsewhere.

SIGNATURE:

DATE:

Supervisor's Declaration



I hereby declare that the preparation and presentation of this work was supervised in accordance with the guidelines for supervision of thesis/dissertation/project as laid down by the University of Education, Winneba.

PROFESSOR EBENEZER BONYAH

SIGNATURE:

DATE:

DEDICATION

I would like to dedicate this work to ALLAH Almighty, the author of knowledge and wisdom for giving me this opportunity to do my Master's degree. He has been the source of my strength and inspiration throughout this program. To my wife and children Shefaw Mohammed Alhassan, Rahima Beninya Alhassan, Anisa Katari Alhassan, Hawa Alhassan and Fawaz Suhuyini Alhassan who were affected by my commitment to the completion of this work.



ACKNOWLEDGEMENT

The completion of this thesis could not have been possible without the assistance of Professor Ebenezer Bonayah. His supervision and contributions are sincerely appreciated and gratefully acknowledged. I also thank Ing. Dr. Koffi Agbeblewu for his contribution and guidance towards the completion of this thesis. To all relatives, friends and others who in one way or another shared their support, either morally, financially and physically, thank you. Above all, to the Almighty Allah for the countless grace.



TABLE OF CONTENTS

DECLARATION.....	ii
DEDICATION	iii
ACKNOWLEDGEMENT	iv
TABLE OF CONTENTS	v
LIST OF TABLES	ix
LIST OF FIGURES	x
LIST OF ABBREVIATIONS	xi
ABSTRACT.....	xii
CHAPTER ONE	1
INTRODUCTION	1
1.1 Background to the Study.....	1
1.2 Problem Statement.....	4
1.3 Objectives of the Study.....	5
1.4 Significance.....	5
1.5 Organization of the Study	6
CHAPTER TWO	7
LITERATURE REVIEW	7
2.1 Conceptual Review	7

2.1.1 The Concept and Historical Development of Antennas.....	7
2.2 Antenna Properties	10
2.2.1 Electrical Modelling of Antenna.....	11
2.2.2 Other Antenna Parameters	15
2.3 Planar Antennas	18
2.3.1 Classes of Planar Antennas	19
2.3.1.1 Patch Antennas.....	20
2.3.1.2 Slot Antennas	21
2.3.1.3 Planar Traveling-wave Antennas (TWA).....	23
2.3.1.4 Microstrip Leaky-wave Antennas.....	24
2.3.1.6 Printed Quasi-Yagi Antennas.....	26
2.4 Broadband Planar Antennas.....	28
2.5 Slot Antenna Review and Development.....	29
2.5.1 Equivalent Circuit of a Slot Antenna	34
2.6 Broadband Circularly Polarized Slot Antennas Theory.....	35
2.7 Single Fed Circularly Polarized Microstrip Antenna (Rectangular Type).....	36
2.7.1 Type A Patch	39
2.7.2 Type B Patch	41
2.8 Theoretical Review	43
2.8.1 The Theory of Characteristic Modes.....	43
2.8.2 Antenna Synthesis.....	44

2.8.3 Performance Requirement of Slot Antennas.....	45
2.9 Empirical Review of Slot Antenna Design and its application.....	45
CHAPTER THREE.....	51
METHODOLOGY	51
3.1 Conceptual Methodology.....	51
3.2 Design Methodology Using HFSS Software	52
Fig. 3.1 Antenna design Flow chart	52
3.3 Antenna Design Procedures	53
3.3.1 Substrate.....	53
3.3.2. Radiator.....	54
3.3.3 A Stab	55
3.4 Simulation Parameters and Processes	64
CHAPTER FOUR.....	68
ANTENNA SIMULATION RESULTS AND DISCUSSION	68
This chapter presents and discusses the various results of the simulation.....	68
4.1 L Slot Antenna Configuration	68
Figure 4- 1 Geometry of the Proposed Antenna. (a) Top side (b) Bottom side	69
Table 4- 1 Antenna Parameters	70
Figure 4.3 Reflection coefficient of antennas I-IV	72

4.2 Parametric Study.....	72
A. The Effect of the Ground stub length (Gst)	72
tion coefficient for antenna IV with different lengths of ground stub (Gst).....	73
B. The Effect of the Feedline Stub length (s)	73
4.3 L Slot Antenna Performance Simulation.....	74
Figure 4.6 simulated results of the proposed antenna. (a) Reflection coefficient, (b)	
Gain	75
Figure 4.7 simulated radiation patterns of the proposed antenna at (a) 5 GHz, (b) 7....	76
GHz (c) 9 GHz (d) 11 GHz	76
Table 4.2 Results Compared to Other Results in the Literature.....	77
CHAPTER FIVE	82
SUMMARY OF FINDINGS, CONCLUSION AND RECOMMENDATIONS	82
5.1 Summary of Findings.....	82
5.2 Conclusion	84
5.3 Recommendations.....	85
REFERENCES	86
APPENDIX	94

LIST OF TABLES

Table 2.1 Summary Characteristic of Selected Types of Planar Antennas	27
Table 4- 1 Antenna Parameters.....	70
Table 4.2 Results Compared to Other Results in the Literature	77



LIST OF FIGURES

Figure 2.1 A Sample Side-Mounted Antenna	9
Fig 2.3a Patch Antenna.....	20
Fig 2.4a Slot Antenna	22
Figure 2.2 (a) Antenna in transmitting mode.....	15
Figure 2.2 (b) Thevenin equivalent	15
Figure 2.2 (c) Transmitting antenna and its equivalent circuits.	15
Figure 2.6: Designed Broadband Planner Slot Antenna (Sakakibara et al, 2012.	29
Figure 2.7 a-b Center fed microstrip slot antenna configurations (a) Microstrip terminated in a short-circuit (b) Microstrip terminated in an open-circuited stub (garg, et al, 2001).	31
Figure 2.8 Two possible ways of reducing input impedance of a slot antenna (a) offset microstrip feeding (b) center-fed but inclined microstrip feed (Garg, et al, 2001).....	32
Figure 2.9 Equivalent Circuit of a Microstrip-Fed Slot Antenna (Balanis 2014).....	34
Figure 2.10 various types of microstrip antenna perturbations for circular polarization generation	37
Fig 2.11 patch and its coordinate system.....	37
Figure 2.12 Configuration of single fed microstrip patch antennas: (a) patch diagram and (b) type A and type B microstrip patch perturbations (Garg, et al, 2001).....	38
Figure 2.13 Equivalent circuit of microstrip patch antenna with perturbation (Garg, et al, 2001).	40
Fig. 3.1 Antenna design Flow chart.....	52
Figure 4- 1 Geometry of the Proposed Antenna. (a) Top side (b) Bottom side	69
Figure 4.3 Reflection coefficient of antennas I-IV	72
Fig 4.4 Reflection coefficient for antenna IV with different lengths of ground stub (Gst) .	73
Fig 4.5 Reflection coefficient for antenna IV with different lengths of feedline stub (s)....	74
Figure 4- 6 simulated results of the proposed antenna. (a) Reflection coefficient, (b) Gain	75
Figure 4- 7 simulated radiation patterns of the proposed antenna at (a) 5 GHz, (b) 7	76
Fig 4.8. Received power over a varying Tx-Rx distances).	79
Fig 4.9. Pathloss over varying Tx-Rx distances.	80

LIST OF ABBREVIATIONS

CPW: Coplanar Waveguide

CWSA: Constant Width Slot Antennas

EMI: **Electromagnetic Immunity**

FDTD: Finite-Difference Time-Domain

FEM: Finite Element Method

GPRS: General Packet Radio Service

HFSS: High-frequency Structure Simulator

IEEE: Institute of Electrical and Electronics Engineers

LLDPE: Linear Low Density Polyethylene

MANET: Mobile ad hoc network

MSAs: Microstrip Antennas

PEC: Perfect Electric Conductors

PIFA: Planar Inverted-F antenna

PIFLA: Planar Inverted F-L Antenna

TCM: Theory Of Characteristic Modes

THz: Terahertz Frequency

TSA: Tapered Slot Antennas

TWA: Traveling-wave Antennas

VHF: Very high frequency

WBAN: Wireless Body Area Network

WiMAX: Worldwide Interoperability For Microwave Access

WLAN: Wireless Local Area Network



ABSTRACT

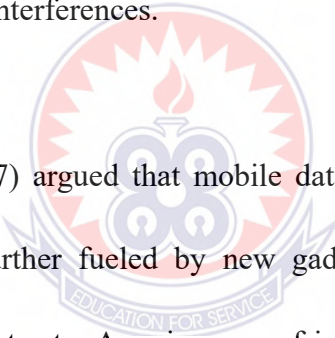
This study aimed at the design and analysis of broadband planar slot antenna for future communication networks such as 5generation wireless communication systems and beyond. The Ansys High-frequency Structure Simulator (HFSS 19) version (2019) is used in the development and simulation modeling of the antenna. The HFSS software is based on the finite element method (FEM) for solving electromagnetic field problems. The main data used in this simulation tool are shapes and dimensions of the desired model as well as feeding techniques. The proposed antenna in this study is the broadband planar slot antenna. It is a compact multiband resonance antenna with very good impedance bandwidth. Consequently, the conception and the simulation of a new low cost rectangular planar antenna is performed based on the theoretical equations to find out the initial antenna dimensions. The study found that the proposed antenna has near stable radiation patterns across the operating bandwidth albeit with high cross polarization patterns in the high frequency range (above 10 GHz) due to the asymmetrical nature of the antenna. A link budget analysis showed that the antenna can work effectively as a WLAN antenna. Again, the path loss is less than 75 dB over the entire 150 m chosen for the analysis. Key recommendations included the need for future work to look into implementing the antenna as a circularly polarized antenna to solve the issues of polarization. It was also recommended that techniques to make the antenna reconfigurable should be explored to avoid the need for extra signal processing circuits to switch between frequencies when the antenna is deployed in a device.

CHAPTER ONE

INTRODUCTION

1.1 Background to the Study

Antennas are transducers that transfer electromagnetic energy between a transmission line and free space. Antennas are reciprocal devices that can be utilized as both transmitting and receiving elements in most cases. Antenna systems are experiencing a renaissance because they have emerged as one of the most important technologies for boosting wireless communication system capacity and data speeds. Their use helps mitigate three major impairments caused by the wireless channel; namely fading, delay spread and co-channel interferences.



Kamal, and Chaudhari, (2017) argued that mobile data have known unprecedented growth. This growth was further fueled by new gadgets namely e-book readers, notebooks, smartphones, tablets etc. A major area of interest that has emerged is the broadband wireless access technologies. The increase in the development of broadband wireless access technologies for evolving wireless, mobile internet service and next generation cellular systems have been significant. These technologies have been developed to be able to cope with the challenging wireless environment and antenna systems in the form of adaptive arrays or smart antennas that can provide an effective and promising solution while achieving a reliable and robust high speed and high data rate transmission (Roh, Seol, Park, Lee, Lee, Kim, &Aryanfar, 2014). A

leading innovation in this regard is the slot antennas. Because of its appealing properties such as low profile, broadband, compact size, light weight, low cost, and ease of manufacture, these antennas are widely used. Furthermore, they are highly compatible with other radio frequency microwave integrated circuits in terms of manufacturing and have a minimal coupling effect in terms of installation. It has been demonstrated that using a combination of antenna geometry and a range of slot shapes to improve, expand the antenna working bandwidth, and adapt the input impedance is a viable option.

The slot antenna, consisting of a narrow slit in a ground plane, is a very versatile antenna. A slot antenna consists of a metal surface, usually a flat plate, with one or more holes or slots cut out. The slot radiates electromagnetic waves in a manner similar to a dipole antenna when the plate is operated as an antenna by an applied radio frequency current. The radiation pattern is determined by the slot's form and size, as well as the driving frequency. Slot antennas are most commonly employed at ultra-high frequency (UHF) and microwave frequencies, when the wavelengths are short enough to make the plate and slot tiny.

Booker (1946) shows that a slot in a metal plate or waveguide has the same radiation pattern as a driven rod antenna whose rod is the same shape as the slot, with the exception that the electric and magnetic field directions are reversed; the antenna is a

magnetic dipole instead of an electric dipole; and the magnetic field is parallel to the slot's long axis and the electric field is perpendicular. As a result, the radiation pattern of a slot may be estimated using the same well-known formulae that are used to determine the radiation pattern of rod element antennas like the dipole. Perpendicular to the slot axis, the waves are linearly polarized. A single main lobe with maximal radiation perpendicular to the surface is present in slots up to a wavelength in length.

Alan Blumlein is credited with the invention of the slot antenna in 1938. He created this invention while working for Electromagnetic immunity (EMI). His goal with this invention was to be able to make a VHF television antenna with horizontal polarization, an omnidirectional horizontal radiation pattern, and a limited vertical radiation pattern that would be practical to use (Burns, 2000). A parabolic segment reflector, or "cheese antenna," was previously utilized in surface search radar systems. During World War II, McGill University and the National Research Council of Canada collaborated on radar research, which resulted in the slotted waveguide antenna (Covington, 1991).

The interest of this study is to design a broadband planar slot antenna. The slot antenna has been employed in all aspects of wireless and radar applications, and evidence suggests that it is suitable to waveguide, coplanar waveguide (CPW), coaxial, slot line, or microstrip feeding schemes with modification. Unlike the

waveguide slot antenna, which is only activated from one side, the planar slot antenna radiates in both directions. Alternatively, to eliminate backside radiation, the slot can be cavity- or reflector-backed, but this adds weight and complexity (Covington, 1991). In this regard, the quest for high bandwidth antennas becomes extremely important.

1.2 Problem Statement

In the last few decades, wireless communication industry has seen rapid growth, with the large number of mobile devices connected to the internet. This brings into desire to use a single device for multiple wireless applications. There are demands to design high performance, high bandwidth multiband antenna that can satisfy the desire of high speed data communication along with device portability (Burns, 2000). Therefore, significant number of engineers and researchers are working to design high performance antennas for various wireless communication applications. The problem is that there have been various antennas proposed in the literature but mostly either they are complex in structure or performance is not good (Burns, 2000). Some are also fraught with challenges such as high link losses, low gain, low or narrow bandwidth, limited coverage and environmental losses.

The theoretical prototype antenna in this study is a broadband planar slot antenna. It is a compact multiband resonance antenna with very good impedance bandwidth and return loss. The reasons for this proposed antenna design is not farfetched. With rapid

development of wireless communication, low profile antenna with good radiation performance are in great demand, especially for wireless local area network (WLAN) and Worldwide Interoperability for Microwave Access (WiMAX) applications, and in space applications such as satellite, aircraft and radar in some military platforms, and future generation x networks (C. Band, X Band). Slot antennas, for their attractive characteristics such as low profile, conformability to planar or curved surfaces, easy integration with planar circuits and better isolation from feed network, are very suitable for these applications and have been extensively studied by many researchers. It is for its unique characteristics that it is being proposed in this study.

1.3 Objectives of the Study

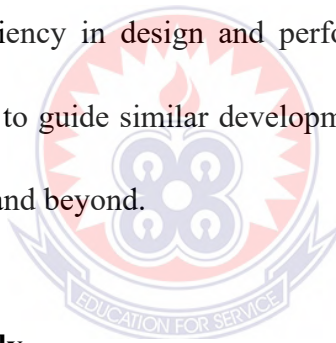
The study aims at developing a compact broadband planar slot antenna for 5th generation communication networks. Specifically, the study will seek to:

- design a broadband planar slot antenna.
- assess techniques to achieve miniaturization of the developed antenna to suit the needs for device specifications.
- evaluate its key parameters such as impedance bandwidth, gain, radiation patterns and efficiency.

1.4 Significance

The study is significant for several reasons. In the first place, it will provide vital

knowledge to industry on the development of broadband antennas. Broadband wireless sits at the confluence of two of the most remarkable growth stories of the telecommunications industry in recent years. The basic requirements for future communication networks is to use a thin antenna. A transmission line's guided electromagnetic wave is converted to a plane wave travelling in free space (transmission) by an antenna, or vice versa (receives). The key advantages of a slot antenna are its small size, simple design, and ease of mass manufacture using waveguide or PC board technology. It is for these features that are being proposed in this study. The study will avail to the industry an alternative to existing antenna designs with improved efficiency in design and performance. The study will also serve as a reference material to guide similar developments in future communication systems, 5th generation (5G) and beyond.



1.5 Organization of the Study

The rest of the study is structured as follows. The chapter two (2) reviews the existing literature related to the study to gain an understanding of the research topic. Chapter three (3) presents the methodology to be used, bringing into perspective the materials and methods, design concepts and approach. Chapter four (4) discusses the design and its output and level of efficiency. Chapter five (5) summarizes the findings of the study and also makes recommendations that would contribute to solving the problem raised, and for further study.

CHAPTER TWO

LITERATURE REVIEW

This chapter focuses on the conceptual, theoretical and the empirical reviewing literature that relates to design and simulate a broadband planar slot antenna and its efficiency.

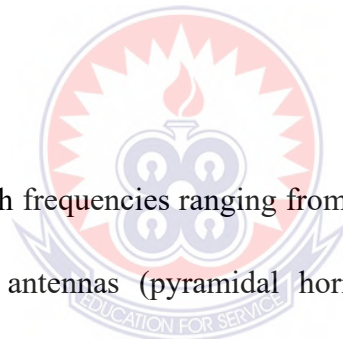
2.1 Conceptual Review

The conceptual review is limited to antennas, with emphasis on the planar antennas in regard to its associated lexica are discussed.

2.1.1 The Concept and Historical Development of Antennas

Antennas have become critical in our regular daily existence. Hiraga (2013) depicts the device as a gadget that is utilized to communicate and get the information as electromagnetic waves as it were. Antennas are by and large defined by the frequencies, low-frequencies, medium-frequencies, and high-frequencies. H. Hertz, a German physicist, proposed low-frequency antennas, such as a dipole antenna, in the first place; nonetheless, it took 20 years to actually erect this antenna. Marconi conducted an experiment using a half-wave dipole to send information from the Atlantic, which was successfully received at the reception side, namely St. John's, Newfoundland. Marconi was the one who successfully sent information using Prof. J.C. Bose's hypothesis. J.C. Bose was later noted for his work on horn antennas (Hiraga, 2013).

As per Radisic (1998), these signal transmissions were restricted to a 200-m distance, and subsequently, De Forester and Felleming created vacuum tubes; this prompted the expansion in transmission distance to 600 m. The development enhanced the role of electrical and electronics devices for long-distance communications. The late 1920s saw the development of the medium-frequency antenna having ranges from 300 to 3000 KHz. This antenna was built utilizing steel bar sustained by means of wooden bars (Li et al, 2007). Following this, there were additional advances and improvements to the antenna until the 1960s, when the medium-frequency antenna was improved, and various antennas were developed that satisfied these ranges (Qian et al, 1999).



High-frequency antennas with frequencies ranging from 0.003 to 40 GHz and beyond were on display. Aperture antennas (pyramidal horn, circular horn, rectangular waveguide), antenna arrays (linear or planar arrays), and reflector antennas (parabolic reflectors with horn fed or Cassegrain feed, lens antenna, and microstrip antennas (MSAs)) are all examples of high-frequency antennas that use a rectangular, square, or circular conducting patch with grounded substrates (Xu and Zhang, 2015). Several antenna types have since emerged with various capabilities and capacities; the planar class of antennas, which is the subject of the study, being one of the very popular types.

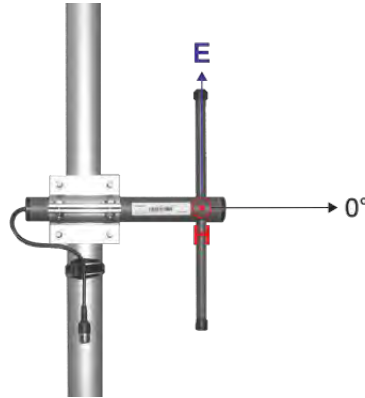


Figure 2.1 A Sample Side-Mounted Antenna

The account by Jeemon et al, (2013) suggests that William Gilbert in A.D. 1600, led the methodical tests of the phenomena of magnetism and electricity by exploring the electroscope for estimating electrostatic impacts and considered the earth as itself a magnet. The relationship between magnetism and electricity was established James clerk Maxwell (1865), who was with the Cambridge University, England. Electricity and magnetism's first theory was published by James C. Maxwell. He also developed the concept of electromagnetism.

Hertz experimented with a spark he created at a dipole's centre and found that a similar spark was received at a gap located in a nearby loop. He subsequently tested and proved that Hertzian waves could be utilized for sending messages. He got the experiment repeated by having big antennas and ground systems tuned for longer wavelengths and was able to have the signal travelling over long distance.

He made a breakthrough in 1901 with radio however at that point it was wireless;

famously known as Marconi's wireless. Monopole antennas (almost quarter wavelength) are generally utilized in Marconi's experiments. Jagadish Chandra Bose the popular Indian researcher produced the 60GHz signals. In the First World War vacuum tubes were accessible for transmission of the continuous waves, and supplanted by sparkle and radio broadcasting started for 200 to 600-meter range. The British and the American researchers added radar innovation to reach the targets from many miles. In this way, research brought about the improvement of high frequency radar antennas, for example, horn antennas.

While the antennas turned into the fundamental part for radio communication, broadcasting and radar systems, the broadband antennas, planar antennas, circularly polarized antennas have opened new period in the advancement of the antennas. Numerous application areas like worldwide interoperability of microwave access (Wi-MAX), wireless local area network (WLAN), Bluetooth, wireless fidelity (Wi-fi), satellite communication, and required diverse antenna to help in future communication networks (5G and beyond).

2.2 Antenna Properties

The presentation of the antennas is dictated by a few components such as impedance bandwidth, gain, radiation patterns and efficiency.

2.2.1 Electrical Modelling of Antenna

Input impedance is essential to decide maximum power transfer between transmission line and the antennas. This transfer possibly happen when input impedance of antenna and input impedance of the transmission line matches. In the event that they don't coordinate, reflected wave will be created at the antenna terminal and travel back towards the energy source. This impression of energy results causes a decrease in the general efficiency of the system (Sharma et al, 2020).

According to Balanis (2016), "The impedance presented by an antenna at its terminals, or the ratio of the voltage to current at a pair of terminals, or the ratio of the appropriate components of the electric to magnetic fields at a location," according to the definition of input impedance. The input impedance at a pair of terminals, which are the antenna's input terminals, is the main focus of this section. In Figure 2.2(a) these terminals are designated as a – b. The ratio of the voltage to current at these terminals, with no load attached, defines the impedance of the antenna as

$$Z_A = R_A + jX_A \quad (2.1)$$

Where $Z_A =$ antenna impedance at terminals a – b ohms)

$R_A =$ antenna resistance at terminals a – b ohms)

$X_A =$ antenna reactance at terminals a – b ohms)

In general the resistive part of (2-1) consists of two components; that is

$$Z_A = R_r + R_L \quad (2.2)$$

Where

$R_r =$ radiation resistance of the antenna

$R_L =$ loss resistance of the antenna

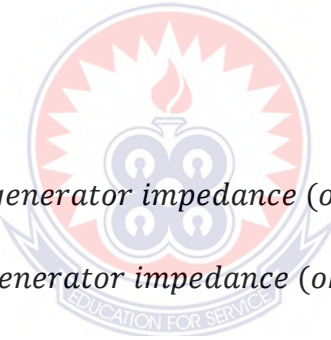
If we assume that the antenna is attached to a generator with internal impedance

$$Z_g = R_g + jX_g \quad (2.3)$$

Where

$R_g =$ resistance of generator impedance (ohms)

$X_g =$ reactance of generator impedance (ohms)



and the antenna is used in the transmitting mode, we can represent the antenna and generator by an equivalent circuit shown in Figure 2.2(b). To find the amount of power delivered to R_r for radiation and the amount dissipated in R_L as heat ($I_2 R_L / 2$), we first find the current developed within the loop which is given by

$$I_g = \frac{V_g}{Z_1} = \frac{V_g}{Z_A + Z_g} = \frac{V_g}{(R_r + R_L + R_g) + j(X_A + X_g)} \quad (2.4)$$

And its magnitude by

$$[I_g] = \frac{[V_g]}{[(R_r + R_L + R_g)^2 + (X_A + X_g)^2]^{1/2}} \quad (2.5)$$

Where. V_g is the peak generator voltage. The power delivered to the antenna for radiation is given by

$$P_r = \frac{1}{2} [I_g]^2 R_r = \frac{[V_g]^2}{2} \left[\frac{R_r}{(R_r + R_L + R_g)^2 + (X_A + X_g)^2} \right] \quad (2.6)$$

And that dissipated as heat by

$$P_L = \frac{1}{2} [I_g]^2 R_L = \frac{[V_g]^2}{2} \left[\frac{R_L}{(R_r + R_L + R_g)^2 + (X_A + X_g)^2} \right] \quad (2.7)$$

The remaining power is dissipated as heat on the internal resistance R_g of the generator, and it is given by

$$P_g = \frac{[V_g]^2}{2} \left[\frac{R_g}{(R_r + R_L + R_g)^2 + (X_A + X_g)^2} \right] \quad (2.8)$$

The maximum power delivered to the antenna occurs when we have conjugate matching; that is when

$$R_r + R_L = R_g \quad (2.9)$$

$$X_A = -X_g \quad (2.10)$$

For this case

$$P_r = \frac{[V_g]^2}{2} = \left[\frac{R_r}{4(R_r + R_L)^2} \right] = \frac{[V_g]^2}{8} \left[\frac{R_r}{4(R_r + R_L)^2} \right] \quad (2.11)$$

$$P_L = \frac{[V_g]^2}{8} = \left[\frac{R_L}{(R_r + R_L)^2} \right] \quad (2.12)$$

$$P_g = \frac{[V_g]^2}{8} = \left[\frac{R_r}{(R_r + R_L)^2} \right] = \frac{[V_g]^2}{8} \left[\frac{R_r}{R_r + R_L} \right] = \frac{[V_g]^2}{8R_g} \quad (2.13)$$

From (2-12)–(2-13), it is clear that

$$P_g = P_r + P_L \frac{[V_g]^2}{8} \left[\frac{R_g}{(R_r + R_L)^2} \right] = \frac{[V_g]^2}{8} \left[\frac{R_r + R_L}{(R_r + R_L)^2} \right] \quad (2.14)$$

The power supplied by the generator during conjugate matching is

$$P_s = \frac{1}{2} V_g I_g = \frac{1}{2} V_g \left[\frac{V_g}{2(R_r + R_L)} \right] = \frac{[V_g]^2}{4} \left[\frac{1}{R_r + R_L} \right] \quad (2.15)$$

Half of the power generated by the generator is wasted as heat in the generator's internal resistance (R_g), while the other half is sent to the antenna. Only when we have conjugate matching does this happen. Portion of the power sent to the antenna is radiated through the mechanism provided by the radiation resistance, while the rest is dissipated as heat, affecting part of the antenna's total efficiency. An antenna's input impedance is usually a function of frequency. As a result, the antenna will only be matched within a bandwidth to the interconnecting transmission line and other connected equipment. Furthermore, the antenna's input impedance is influenced by a variety of parameters, including its geometry, manner of excitation, and proximity to nearby objects. Only a small number of practical antennas have been studied analytically due to their complicated geometry. The input impedance of several others has been determined experimentally.

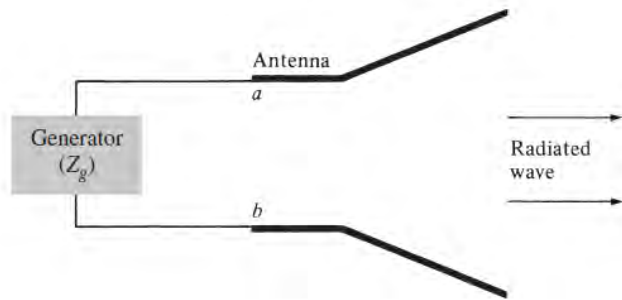
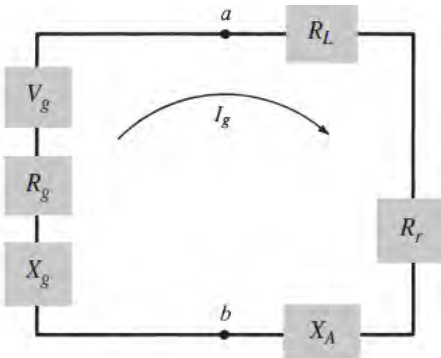
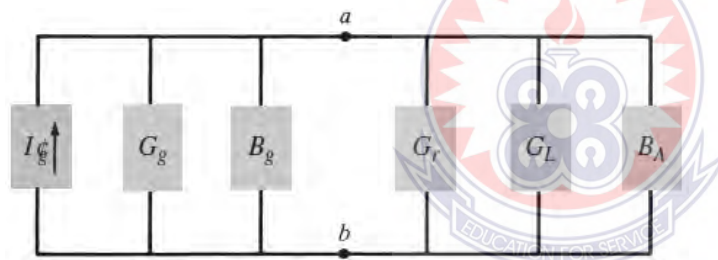


Fig 2.2 (a) Antenna in transmitting mode



(b) Thevenin equivalent

Fig 2.2 (b) Thevenin equivalent



(c) Norton equivalent

Figure 2.2 (c) Transmitting antenna and its equivalent circuits.

2.2.2 Other Antenna Parameters

Other antenna parameters include gain, radiation pattern, directivity, polarization and bandwidth.

An antenna's gain is basically a proportion of the antenna's general efficiency. In the event that an antenna is 100% efficient, it would have an increase equivalent to its directivity. There are many variables that effect and diminish the antenna's overall

efficiency. Probably the main factors include impedance matching, network losses, material losses and arbitrary losses. By thinking about all components, apparently the antennas should beat a ton of difficulty to accomplish satisfactory performance in gain (Sharma et al, 2020).

Meanwhile, the Radiation Pattern (RP) gives the data that depicts how the antenna coordinates the energy it emanates. All antennas if 100% productive, will emanate a similar absolute energy for equivalent input power irrespective of the pattern shape. Radiation designs are by and large introduced on a relative power dB scale (Hiraga, 2013).

On the other hand, Directivity, D is significant feature that shows the capacity of the antennas having radiated energy focused. Directivity is the proportion of maximum radiated to radiate reference antenna. Reference antennas for the most part are an isotropic radiator where the energy radiated is same toward all paths and has directivity of 1. Directivity is characterized by the equation (2.16) :

$$D = \frac{F_{max}}{F_0} \quad (2.16)$$

Where, F_{max} is the Maximum radiated energy, and F_0 the Isotropic radiated energy

It will be noted that Polarization portrays the direction and feeling of the transmitted wave's electric field vector. There are three sorts of fundamental polarization, which

are linear polarization, elliptical polarization, and circular polarization. Generally most antennas transmit with linear or circular polarization. Antennas exhibiting linear polarization radiate at a similar plane with the direction of the wave propagate. For circular polarization the antenna radiate in circular form.

Bandwidth characterizes the frequency range over which an antennas meets a specific set of performance standards. The significant issue to consider with respect to bandwidth is the presentation tradeoffs between the entirety of its exhibition properties portrayed previously. There are two techniques for processing the bandwidth of an antenna.

•
An antenna is considered broadband if:

$$f_H/f_L \geq 2 \quad (2.17)$$

Narrowband by percentage

$$BW_p = (f_H/f_L)/f_0 \times 100\% \quad (2.18)$$

Broadband by ratio

$$BW_p = f_H/f_L \quad (2.19)$$

Where

$f_0 =$ Operating frequency

$f_h =$ Higher cut – off frequency

$f_l =$ Lower cut – off frequency

2.3 Planar Antennas

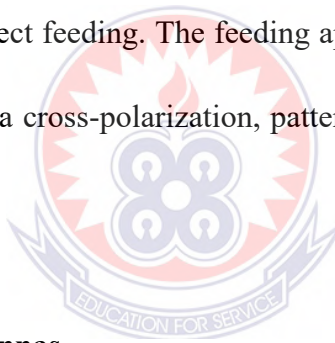
Planar Antennas have received significant attention in the last few decades. The reasons for this increased focus are not farfetched. These antennas are exceptionally attractive for various reasons. In the first place, they can be produced at a much lower cost than waveguide-based antenna innovation and are impressively more reduced and lightweight. These attributes are fundamental for the numerous business applications that planar antennas are progressively utilized in, like base station or handset antennas (Kerketta, 2012).

Second, the planar idea of the antennas makes them ideal for enormous exhibits and improves on the association of extra gadgets, for example, phase shifters and amplifiers, which are fundamental for electronic warfare, radar, satellite interchanges or millimeter-wave imaging. As per Pazar (1992), their planar nature additionally permits the antennas to be utilized in applications where size and shape are pivotal, for example, conformal printed antennas on a plane fuselage. Rebeiz (1992) believes that this bunch of uses has prompted the improvement of a wide assortment of planar antenna classes.

Cui and Fu (2014) point out that one driving element that makes planar incorporated antennas so attractive is their simplicity of mix with microwave or millimeter-wave circuit parts. As a result of these advancements, planar coordinated antennas, which are typically microstrip or coplanar waveguide (CPW) based at microwave and

millimeter-wave frequencies, should be practical. These transmission lines enjoy a few benefits, including the capacity to coordinate three-terminal gadgets, mechanical and heat-sinking abilities because of metallic ground planes and improved issues of packaging.

Henceforth, it is fundamental that these kinds of transmission lines straightforwardly feed the planar incorporated antennas. Instances of direct feeding incorporate the patch antenna and slot antennas, which are handily coordinated with microstrip or CPW, separately (Cui and Fu, 2014). Advances or different types of electromagnetic coupling can be used in indirect feeding. The feeding approach is fundamental, and it has the ability to alter antenna cross-polarization, patterns, and bandwidth, as well as cluster models.



2.3.1 Classes of Planar Antennas

It must be emphasized, for the purpose of this study, that the sloth class of planar antennas is the focus.

Planar antennas have a distinct appearance. Planar antennas of this sort can handle a wide range of radiation properties. Patch and resonant slot antennas, the most well-known classes, have expansive, low-increase designs that make them suitable for usage in multi-component beam forming arrays or adaptable handsets (Oteng and Guangjun, 2002). Moreover, a portion of these antennas can be altered effectively for

dual linear or circular polarization. More refined classes show higher additions and some are fit for frequency filtering. Patch antennas, slot antennas, Microstrip Leaky-wave Antennas, and Planar Traveling-wave Antennas (TWA) are some of the numerous types of planar antennas (Hiraga (2013)).

2.3.1.1 Patch Antennas

There are several advantages to using a patch antenna. The broadside radiation architecture of this antenna allows it to be coordinated into two-dimensional arrays. Moreover, different feeding plans can be utilized to accomplish linear or circular polarization. A cross section of patch antennas is depicted in Figure 2.3. The transmission line model is a simple and intuitive way to demonstrate this antenna. This model assumes that the patch antenna's cavity has perfect magnetic conducting walls on both sides, resulting in standing-wave-type modes. Because of the microstrip open-end impact, the cavity's overall length equals the length of the patch antennas plus a compelling length at each edge. At a frequency where the cavity length is one-half wavelength, the antenna's core resonance occurs.

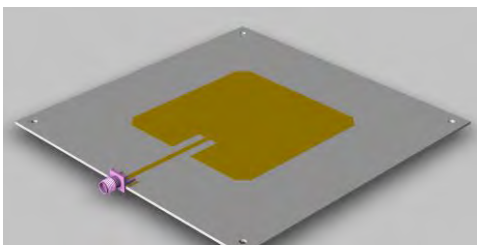


Fig 2.3a Patch Antenna



Fig 2.3b View of a Mounted Patch Antenna

Higher antenna resonances harmonize with frequencies that are products of the basic reverberation since its length determines the patch's resonant frequency (Sharma et al, 2020). Harmonic radiation and co-site blocking may occur if active is coordinated with patch antennas, according to Li et al (2007). The circular segment patch antenna, as well as the measured input, were designed specifically to address this issue (Radisic et al, 1998). In this case, circular harmonics are utilized to manage the antenna's higher resonances and are designed to occur independently of circuit harmonics. This antenna is made of RT/Duroid with a low permittivity.

2.3.1.2 Slot Antennas

Chen (2003) portrays the slot antenna as an exceptionally flexible antenna, made up of a thin cut in a ground plane. With some alteration, the gadget is amiable to waveguide, CPW, coaxial, slotline or microstrip schemes of feeding and has been applied in all parts of remote and radar frameworks (Shin, et al, 2005). The slot antenna has been examined since the 1940s (Booker, 1946). Yoshimuar (1972) alludes to planar microstrip-fed slot antenna being developed since 1972.

The size of the resonant half-wavelength slot antenna makes it desirable. Nonetheless, the antenna has a huge input impedance, ordinarily bigger than 300 W, which makes it not so attractive to match to. In any case, Chen et al (2006) claim that using an offset microstrip feed or the folded slot antenna, which is derived from the folded dipole, this match issue can be avoided. For this situation, the slot antenna is folded in on

itself. The general length of the antenna remains around a half-wavelength, however expanding the quantity of folds lessens the radiation resistance.

The folding slot antenna's CPW adaption has been thoroughly investigated (Ge et al, 2004). These antennas do not require input matching, making them a low-cost and viable option for microwave circuit integration. This antenna's wide radiation pattern also makes it a viable option for wireless communication systems that are currently driving into the microwave system. Figure 2.4 depicts the fundamental structure of a microstrip-fed folded-slot antenna.

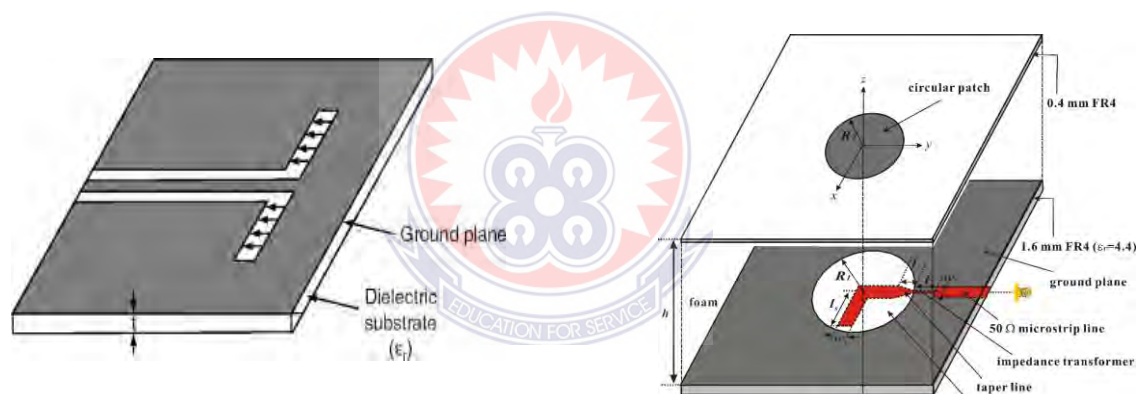


Fig 2.4a Slot Antenna

Fig 2.4b Broadband Slot Antenna

A folded-slot antenna is etched into the substrate's ground plane. A shorting wire connects one of the slot's inner metallizations to the microstrip conductor on the top plane. With a permittivity of 2.33 and a substrate thickness of 31 mils, a two-folded slot on an RT/Duroid substrate may easily achieve a 50 W input impedance. The slot operation may be visualized easily using the FDTD simulation. The feeding system is

clearly working and the fields are being directed across the slot as anticipated. At the slot's edges, perpendicular fields exist, contributing to the radiated fields' cross-polarization. According to simulations, lowering the space at the slot's edges reduces cross-polarization while sacrificing bandwidth (Kerketta, 2012).

2.3.1.3 Planar Traveling-wave Antennas (TWA)

Resonant type (or standing-wave) antennas, including the patch and slot antennas, regularly have restricted bandwidth and somewhat basic, unobtrusive gain radiation patterns. Another class of antennas - travelling wave - contains structures that radiates with the propagation of the waves. These designs are electrically huge when contrasted with resonant type structures, and regularly exhibit higher gain. They likewise may create expansive performance in broad bandwidth. TWA's regularly are partitioned into two classes: leaky wave and surface wave.

The leaky-wave antenna continuously radiates as the wave spreads; the surface-wave antennas radiates within the structures at points where discontinuities gets the propagating surface wave disrupted and normally is a lethargic wave structure. The capacity to design a wide assortment of planar transmission line and surface-wave structures implies that great planar variants of these antennas might be created. Notwithstanding, it is accepted that work in this slot is a long way from develop and numerous potential outcomes still need to be explored (Saed, 2006).

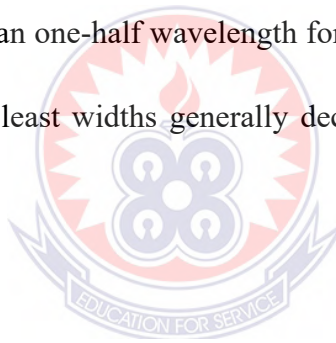
2.3.1.4 Microstrip Leaky-wave Antennas

A higher order radiative microstrip mode is used to shape a leaky wave antenna in this type of leaky-wave antenna. The symmetry of the radiation mode is odd and tops at the edges of the microstrip cross area with the center having a null. Hence, as the signal is propagated along the transmission line of the microstrip, energy radiates ceaselessly along the edges, bringing about the main radiation beam. If the structure's end isn't finished, the remaining energy will be reflected from the open end, resulting in a subsequent beam.

For long antennas, the measure of force reflected from the open end will be little, bringing about a more modest second beam. Moreover, the main beam's direction happens as a component of frequency, permitting the likelihood that the antenna can be frequency examined. Notwithstanding, the microstrip leaky wave just radiates effectively over a bandwidth that is fixed, which, by and by, limits scanning at maximum. Moreover, the antenna's feeding and length likewise have some impact on the pattern. A microstrip leaky-wave antenna which is aperture-coupled and having a broadside-directed beam has previously been reported (Saed, 2006). Getting such an antenna fed is a major concern, and different schemes have been reported. In essence, the higher order leaky-wave mode must be excited with minimal basic mode stimulation (Kumarasamy, 2017).

2.3.1.5 Tapered Slot Antennas

A lot of research has recently been done on tapered slot antennas (TSA) on dielectric substrates. These are planar systems, have an end fire design and are equipped for getting high directivity as well as bandwidth. Millimeter-wave imaging, power consolidation, and usage as a working coordinated antenna component are among the applications proposed. On one side of a dielectric substrate, the TSA is etched into the metallization. Normally, the dielectric constant is low. The Vivaldi, linear TSA (LTSA), and constant width slot antennas are three well-known layouts (CWSA). Where the slot has a specified diameter, a specific frequency of radiation occurs. Slot width should reach no less than one-half wavelength for effective radiation to happen. In this manner, greatest and least widths generally decide the structure's bandwidth (Xu and Zhang, 2015).

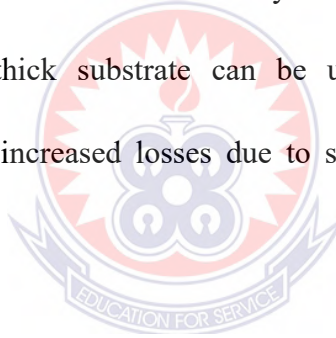


In order to achieve acceptable radiation patterns and maintain high radiation efficacy, TSAs are typically built on sparse, low permittivity substrates, which are reduced by TM₀ surface-wave losses. Micromachining has been used to reduce the electrical thickness of millimeter-wave TSAs by decreasing the permittivity, similar to patch antennas. This development allow a truly thicker substrate, which is fundamental for mechanical help for this sort of structure at millimeter wavelength. Also, when utilized as an antenna that is integrated, a change from the preferred transmission line (regularly, microstrip or CPW) should be utilized. The transition's bandwidth might

restrict the structure's bandwidth.

2.3.1.6 Printed Quasi-Yagi Antennas

Planar adaptations of wire antennas such as the dipole, loop, or spiral antenna are printed wire antennas. Due to the prominence of microstrip and coplanar waveguide transmission lines at these frequencies, which are difficult to integrate with wire-based antennas, only limited success has been made in constructing workable versions of completely planar wire antennas. Due to the shorting effect of the microstrip ground plane, a printed microstrip dipole, for example, has a very low radiation resistance and, as a result, will have low efficiency when accurate losses estimations are done. An electrically thick substrate can be used to compensate for this shortcoming (at the cost of increased losses due to substrate waves and increased weight and cost).



Alternatively, the printed wire antenna can be accommodated by modifying the microstrip ground plane. A new sort of microstrip-compatible planar endfire antenna has recently been discussed, based on the well-known Yagi-Uda antenna. A driving element, reflector, and one or more directors make up the classic Yagi-Uda antenna. The parasitic elements are the reflector and the directors (Xu and Zhang, 2015). The antenna features an endfire pattern and a strong gain, although its bandwidth is often limited.

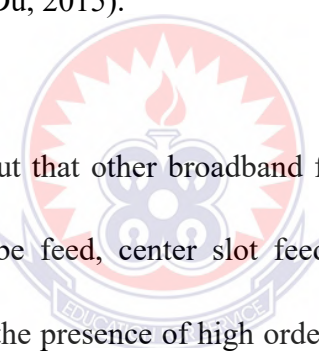
In conclusion, planar antennas come in a variety of shapes and sizes. Patch and slot antennas, for example, are low-profile and compact resonant antennas that can easily be combined into large, active arrays. The wide patterns of the antennas make them helpful in mobile phones as well. Other more unusual planar antennas, such as the microstrip leaky wave, have stronger directivity and frequency scanning capabilities. The quasi-Yagi antenna exemplifies the unexpected amount of functionality that planar antennas may provide. Its small size, wide bandwidth, and superb patterns make it a feasible alternative to existing antenna systems. The functionality of planar antennas is predicted to improve as the technology matures, allowing commercial wireless communications to penetrate increasingly higher frequency applications. The features of the antennas given are summarized in table 2.1, which includes their pattern, directivity, polarization, and bandwidth.

Table 2.1 Summary Characteristic of Selected Types of Planar Antennas

<i>Antenna Type</i>	<i>Pattern</i>	<i>Directivity</i>	<i>Polarization</i>	<i>Bandwidth</i>	<i>Comments</i>
Patch	broadside	medium	linear/circular	narrow	easiest design
Slot	broadside	low/medium	Linear	medium	bidirectional
Ring	broadside	medium	linear/circular	narrow	feeding complicated
Spiral	broadside	medium	linear/circular	wide	balun and absorber
Bow-tie	broadside	medium	Linear	wide	same as spiral
TSA (Vivaldi)	endfire	medium/high	Linear	wide	feed transition
Yagi slot	endfire	medium	Linear	medium	two-layer design
Quasi-Yagi	endfire	medium/high	Linear	wide	uniplanar, compact
LPDA	endfire	medium	Linear	wide	balun, two layer
Leaky Wave	scannable	high	Linear	medium	beam-steering, beam tilting

2.4 Broadband Planar Antennas

Broadband antennas with $>50\%$ bandwidth ($|S_{11}| < -10$ dB), such as Vivaldi antennas (Xu and Zhang, 2015), horn and dish antennas, have a large profile in the direction of wave propagation. Other broadband antennas, such as the planar monopoles, disc cone and slot antennas, have a lower profile, but their radiation patterns are omnidirectional or bidirectional. Broadband patch antennas, such as the E-shaped and U-slots patches [10] using probe feed, have a wide impedance bandwidth of less than 50% for $|S_{11}| < -10$ dB. To lower the Q-value, the dielectric substrates are replaced by air. They are suspended at a height of approximately $0.06-0.1 \lambda_0$, where λ_0 is the free space wavelength (Wang and Du, 2015).



Wang and Du (2015), point out that other broadband feeding techniques include the aperture coupled feed, L-probe feed, center slot feed, suspended probe feed, and folded feed. However, due to the presence of high order modes, the radiation patterns of a patch antenna at higher frequencies are frequently squinting. The patch's volume is expanded to extend the impedance bandwidth, but the high feed inductances from the lengthy feeding probe make impedance matching challenging. Using a single patch radiator and a simple feeding mechanism, designing a broadband planar antenna with >50 percent impedance bandwidth, non-squinting radiation pattern, and a generally constant gain profile (1.5 dBi) is a problem.

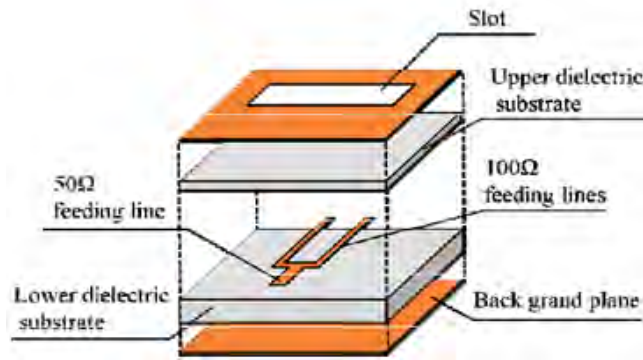


Figure 2.6: Designed Broadband Planar Slot Antenna (Sakakibara et al, 2012).

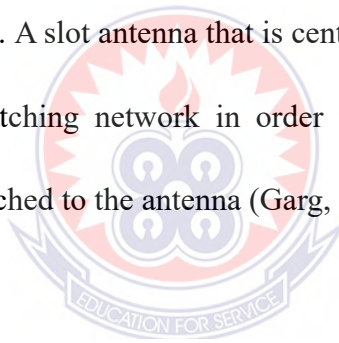
2.5 Slot Antenna Review and Development

Slot antennas as a concept, was invented based on the idea of a strip line. These radiating slots come with the key advantage of having fewer interactions through surface waves, radiation from feed network that is negligible, wider bandwidth, and better isolation (Masoud et al, 1993). Combining slot and strip provides extra design freedom for microstrip antennas and enables it to produce radiation that is circularly polarized (Ito et al, 1979; Ito et al, 1980). Compared to the microstrip patch antennas, the slot antenna concept facilitates the production of antennas with the preferred polarization and show less sensitivity to manufacturing tolerances (Huang & Boyle, 2008).

Slot antennas belong to the aperture-type antennas, and are considered very special. Apart from being low-profile, slot antennas can be configured to any desired specification. This has made them very suitable for various applications, including missiles and aircrafts. Using a waveguide or a coaxial transmission line, slot antennas

can be energized conveniently (Huang & Boyle, 2008). Microstrip slot antenna uses a slot that is cut in the ground plane of a microstrip line in a way that makes the slot perpendicular to the microstrip line's strip conductor. The microstrip line's fields excite the slot.

To get the excitation of the slot to be efficient, there is termination to the strip conductor at the edge of the slot. The strip conductor can also be terminated beyond the slot's edge in a stub that is open-circuited. The open-circuited microstrip stub's length L_m is about a quarter wave length, enabling the realization of an effective short circuit at the slot's outer edge. A slot antenna that is center-fed is resistant to very high radiation and requires a matching network in order to have the microstrip line's characteristic impedance matched to the antenna (Garg, et al, 2001).



Kim and Park (1998) refer to three ways to decrease the resistance seen by the feedline for any given slot size. Yoshimura (1972) proposes the off-center feeding as the first option (See Figure 2.7 (a)). Pozar (1986) describes the process of stub tuning of the slot antennas as another technique. Aside the length microstrip stub's length L_m being longer than that of a quarter wave, this technique is similar to the first technique. The resonant frequency is changed through the stub-tuning due to the introduction of reactive loading of the antenna. The design of the stub to allow input resistance compare with e feedline impedance at the new resonant frequency. The third

technique of feeding is feeding the slot at the center at an inclined position (depicted by 2.7(b)). This technique bears some semblance to the technique used in the waveguide slot antennas.

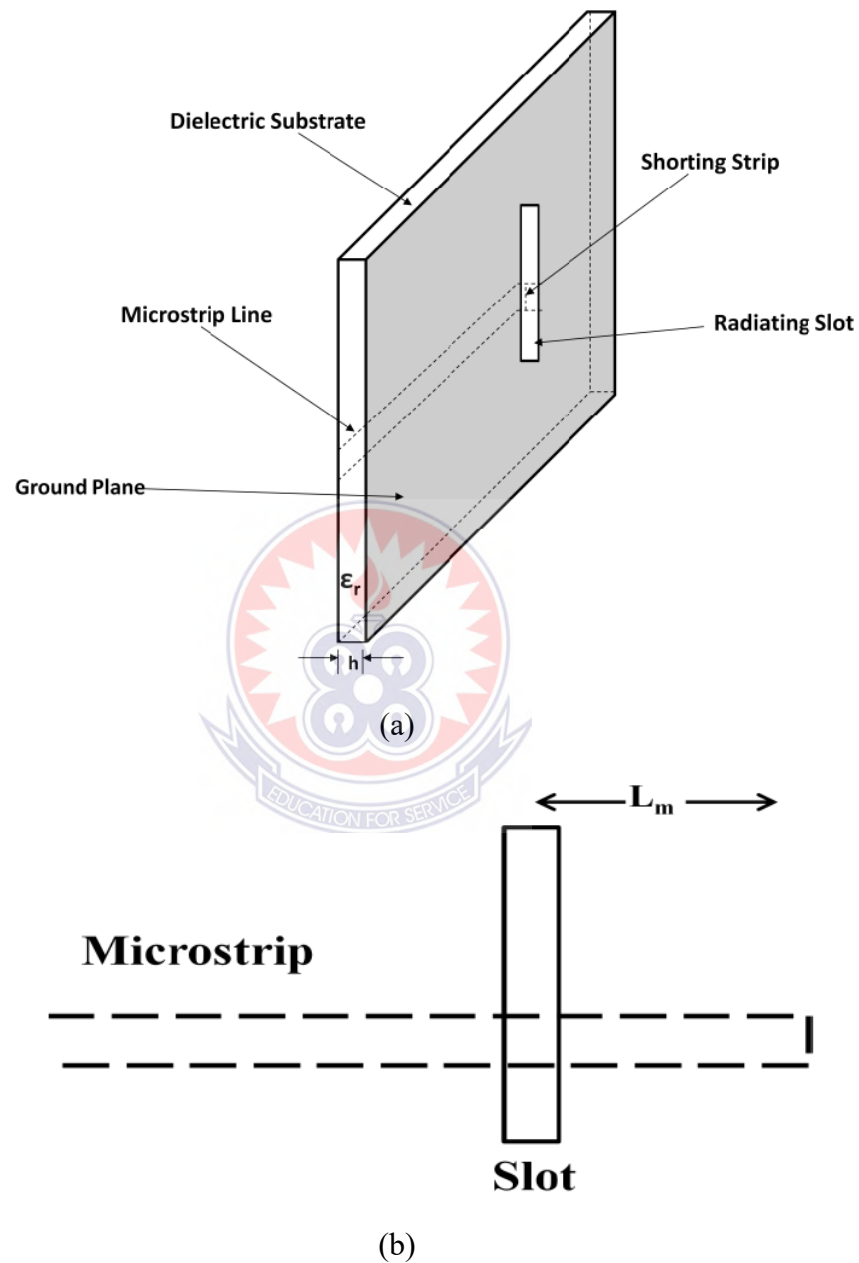


Figure 2.7 a-b Center fed microstrip slot antenna configurations (a) Microstrip terminated in a short-circuit (b) Microstrip terminated in an open-circuited stub (garg, et al, 2001).

Previous studies have proposed network models to assist in the design of efficient slot antennas. The work of Axelrod et al. (1989) modeled the microstrip-slot junction using a transformer considered ideal, expressing the power the slot radiated in the form of an equivalent radiation resistance and located at the center of the slot. The work of Himdy and Daniel (1992) used a lossy transmission line model and the power radiated to find the attenuation constant, radiation conductance and the power radiated of the slot.

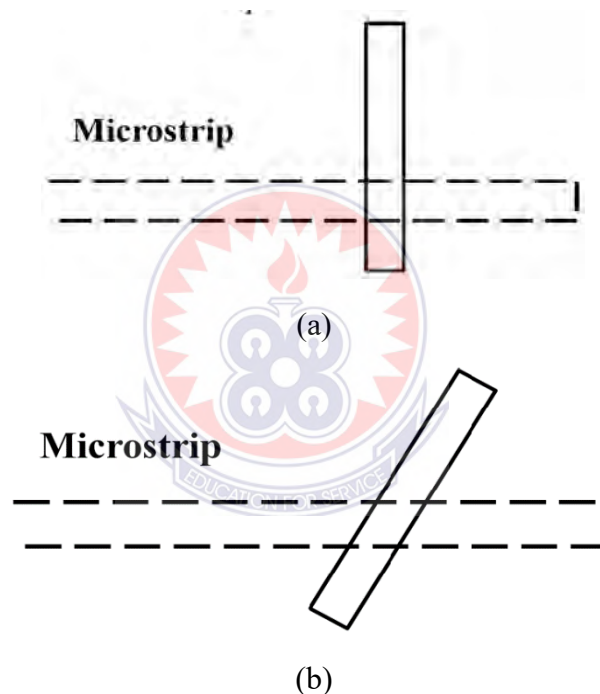


Figure 2.8 Two possible ways of reducing input impedance of a slot antenna (a) offset microstrip feeding (b) center-fed but inclined microstrip feed (Garg, et al, 2001)

Akhavan and Mirshekar-Syahkal (1994) developed an approximate model using a standard expression for the radiation conductance of a resonant slot without a dielectric substrate and approximately determined the self and mutual inductances of the transformer. The work of Kim and Park (1998) also looked at developing a

network model of a microstrip-fed slot antenna that is accurate, off-centered and inclined. Coupled integral equations were formulated by Masoud et al (1993) to ascertain the electric current distribution on the feedline and the electric field in the aperture of a radiating slot that is wide and placed in a microstrip antenna's ground plane. Gupta, et al, (1996) state that series load impedance Z in the microstrip line are used to represent slot antennas. The impedance is a key parameter of any antenna. Babinet's principle asserts that if the field at any position behind a plane with a screen is added to the field at the same point when the complementary screen is substituted, the field at the point when no screen is present equals the field at the point when no screen is present. Huang and Boyle (2008) point out that having this principle applied to antennas and radio propagation using the equivalent transmission line model can help obtain the important relationship for the input impedances of complementary antennas as indicated

$$Z_{slot}Z_{dipole} = \frac{\eta^2}{4} \quad (2.20)$$

The implication of this is that multiplying the impedances of two complementary antennas results in the constant $\eta^2/4$ and this is the version of Babinet's principle in antennas. Since the impedance for a half-wavelength dipole is about 73 ohms, the corresponding slot has an impedance of (Huang & Boyle, 2008)

$$Z_{slot} = \frac{\eta^2}{4Z_{dipole}} = \frac{377}{4 \times 73} \approx 486 \Omega \quad (2.21)$$

Antenna array are formed for practical applications like radars from slot antennas that

have both the feed line and the antenna incorporated and demonstrate capacity for high power handling.

2.5.1 Equivalent Circuit of a Slot Antenna

Kim and Park (1998) posit that it is possible to analyse the microstrip fed slot antenna as a microstrip line discontinuity antenna and described by an equivalent circuit as shown in Figure 2.9. It is composed of a slot line terminated by short circuit at two ends, an ideal transformer, and a radiation conductance. Besides, the slot is seen as two parallel connected sections of slot line with characteristic impedance Z_s and phase constant β_s . Radiation conductance G_r accounts for the power that radiates from the slot. The slot's effective length is taken as $L_s + \Delta L_s - L_c$, where L_s is the physical length of the slot and ΔL_s is the equivalent length associated with the nonzero inductance at the two shorted ends of the slot. A compensation length L_c is introduced to account for the proximity effect of the microstrip line on the slot without using a complicated expression for the slot voltage. This length describes the variation in the observed resonant frequency with microstrip width, substrate parameters, offset distance d , β_s , and turns ratio n of the transformer.

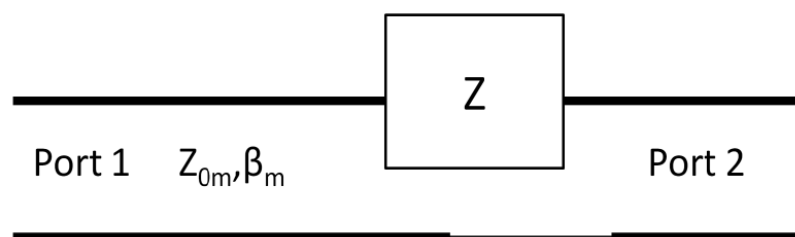


Figure 2.9 Equivalent Circuit of a Microstrip-Fed Slot Antenna (Balanis 2014).

The ideal transformer represents the coupling between the slot and the microstrip line and determines the amount of slot voltage coupled in series to the microstrip. This voltage is also called the discontinuity voltage. The turns ratio n of the transformer is defined as $n = \Delta V_m / V_s$, where ΔV_m is the voltage discontinuity on the microstrip line and V_s is the voltage across the slot at the feed point (Garg, et al, 2001).

2.6 Broadband Circularly Polarized Slot Antennas Theory

The elliptically polarized waves that are generally radiated by antennas are defined by three parameters which include sense of rotation, tilt angle, and axial ratio. Polarization becomes linear with the orientation being defined by the tilt angle when the axial ratio is zero or infinite. The level of cross polarizations usually specifies linear polarization's quality. Regarding the unity axial ratio, there is no use for an ideal circular polarization results and the tilt angle. Overall the axial ratio is utilized to show the nature of circularly polarized waves.

Circularly polarized waves are produced by antennas when two orthogonal field components having the same amplitude however in phase quadrature are radiated. Different antenna wires are fit for fulfilling these prerequisites. They can be gathered as a resonator and traveling wave types. A resonator-type antenna comprises of a single patch antenna that is able to simultaneously support two orthogonal modes in phase quadrature or an array of linearly polarized resonating patches with proper phasing and orientation. An antenna which is the travelling wave type is typically

developed from a microstrip transmission line. It generates circular polarization by having orthogonal components radiated with suitable phasing along discontinuities (Garg et al, 2001).

A microstrip antenna can be described as an antenna that is a resonator type. It is by and large intended for single mode activities that for the most part have linear polarizations radiated. For a circular polarization radiation, orthogonal fields with magnitudes that are equal, however in-phase quadrature, must be supported by a patch. This necessity can be accomplished by a single patch with appropriate excitations or by a variety of patches with reasonable phasing and arrangement. Two kinds of schemes of feeding can be utilized to accomplish circular polarization. The principal type is a feed that is dual-orthogonal, which requires the utilization of an outside power divider network. Garg et al (2001) describe the second as a single-point feed which doesn't need the utilization of an external power divider. Presented below are the design calculations and considerations for a microstrip antenna that is single fed circularly polarized.

2.7 Single Fed Circularly Polarized Microstrip Antenna (Rectangular Type)

The following derivation is for different types of perturbations. They have been grouped into type *A* and type *B* depending on the feed location. From Figure 2.10, it is observed that type *A* patches have the feed located on either the *x*- or *y*-axis, whereas in type *B*, the feed is placed on the diagonal axis of the patch. It is worth noting that

the feed is always located diagonal to perturbation segments that are suitably selected to produce two orthogonally degenerate modes in the patch for CP radiation.

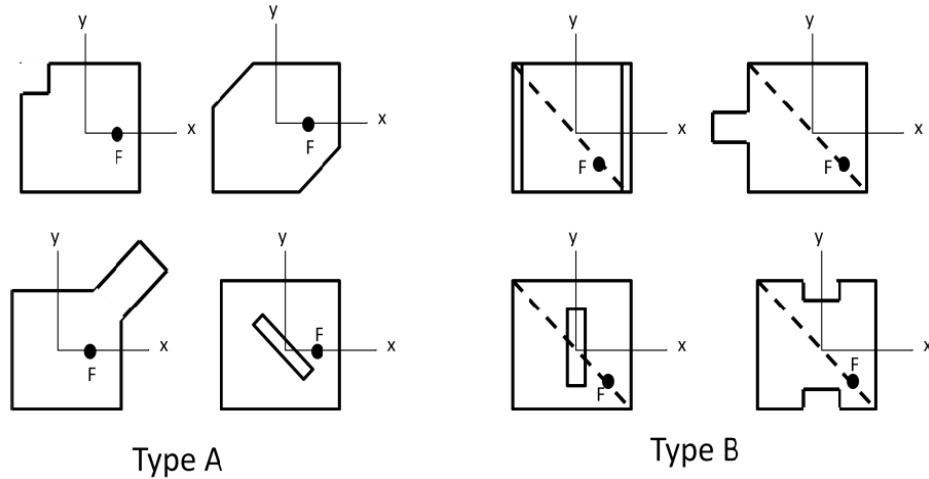


Figure 2.10 various types of microstrip antenna perturbations for circular polarization generation.

The basic configuration of the patch and its coordinate system are shown in Figure 2.11. The square patch is considered to be an electrically thin cavity with perfect magnetic walls at the boundaries, $x = \pm a/2$ and $y = \pm a/2$. In the Figure 2.11, F is the feed point and ΔS represents the total sum of the perturbation segments and may consist of single or multiple segments.

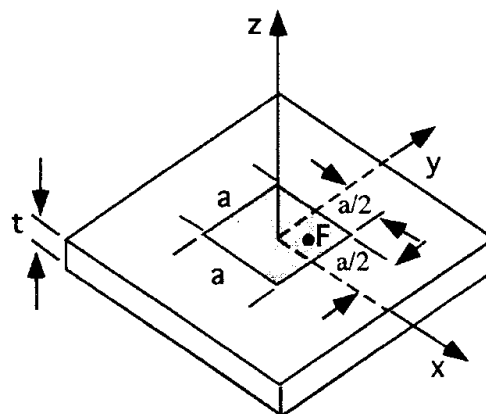
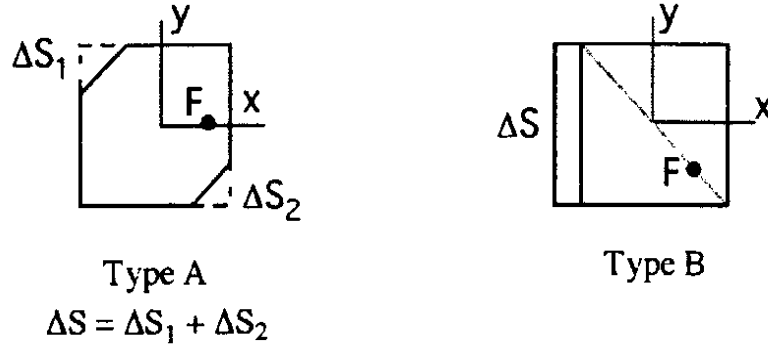


Fig 2.11 patch and its coordinate system

(a)



(b)

Figure 2.12 Configuration of single fed microstrip patch antennas: (a) patch diagram and (b) type A and type B microstrip patch perturbations (Garg, et al, 2001).

The introduction of perturbation segments will affect the cavity model field and its Eigen value, which can be determined from a stationary formula given by:

$$k'^2 = \frac{\int_{S+\Delta S} \nabla \phi' \cdot \nabla \phi' dS}{\int_{S+\Delta S} \phi'^2 dS} \quad (2.22)$$

where ϕ' and k' are the new model field and the new Eigen value. ϕ' can be expanded as

$$\phi' = P\phi_a + Q\phi_b \quad (2.23)$$

where P and Q are unknown expansion coefficients that have to be determined to make (2.22) stationary. Substituting (2.23) into (2.22) results in:

$$k'^2 = \frac{\int_{S+\Delta S} (P\nabla\phi_a + Q\nabla\phi_b) \cdot (P\nabla\phi_a + Q\nabla\phi_b) dS}{\int_{S+\Delta S} (P\phi_a + Q\phi_b)^2 dS} = \frac{U(P,Q)}{V(P,Q)} \quad (2.24)$$

Following the Ritz-Galerkin method, P and Q can be found from

$$\begin{aligned} \frac{\partial U(P,Q)}{\partial P} - k'^2 \frac{\partial V(P,Q)}{\partial P} &= 0 \\ \frac{\partial U(P,Q)}{\partial Q} - k'^2 \frac{\partial V(P,Q)}{\partial Q} &= 0 \end{aligned} \quad (2.25)$$

Equation (2.22-2.25) will result in a set of homogeneous equations that have nontrivial solutions only if the determinant disappears. Exact parameters of the determinant depend on the type of feed and perturbation placements. It can be written generally as

$$\det \begin{vmatrix} k^2 + q_1 - k'^2(1 + p_1) & q_{12} - k'^2 p_{12} \\ q_{12} - k'^2 p_{12} & k^2 + q_2 - k'^2(1 + p_1) \end{vmatrix} = 0 \quad (2.26)$$

2.7.1 Type A Patch

For the type A-fed patch, ϕ_a and ϕ_b are the two normalized degenerate modes, TM_{100} and TM_{010} , of a thin patch which can be written as

$$\begin{aligned} \phi_a &= V_0(kx) \\ \phi_b &= V_0(ky) \end{aligned} \quad (2.27)$$

where $V_0 = \sqrt{2}/a$, $k = \pi/a$, and a is patch size. Using (2.27) in (2.24), all other parameters in (2.25) can be obtained from (2.24) as

$$q_1 = q_2 = q_{12} = 0 \quad (2.28a)$$

$$p_1 = p_2 = 2 \left(\frac{\Delta S}{S} \right) \quad (2.28b)$$

$$p_1 = p_2 = 2 \left(\frac{\Delta S}{S} \right) \quad (2.28c)$$

Substituting equations (2.28a-c) into (2.25), the new Eigen values k'_a and k'_b for the model fields ϕ_a and ϕ_b can be found from (2.24-2.25) as

$$k'^2_a = k^2 \left(1 + 4 \frac{\Delta S}{S} \right)^{-1} \quad (2.29a)$$

$$k'^2_b = k^2 \quad (2.29b)$$

from which the new resonant frequencies of ϕ'_a and ϕ'_b modes are obtained as:

$$f_a = f_{0r} + \Delta f'_a = f_{0r} \left(1 - 2 \frac{\Delta S}{S} \right) \quad (2.30a)$$

$$f_b = f_{0r} + \Delta f'_b = f_{0r} \quad (2.30b)$$

Where f_{0r} is the resonant frequency of the square patch before perturbation, $\Delta f'_a$ and $\Delta f'_b$ are shifts in resonant frequencies for ϕ'_a and ϕ'_b modes after perturbation. Once the new Eigen values k'_a and k'_b are found, expansion coefficients P and Q can be determined from the original set of homogeneous equations and are given by

$$P_a = -Q_a = \frac{1}{\sqrt{2}} \quad (2.31a)$$

$$P_b = Q_b = \frac{1}{\sqrt{2}} \quad (2.31b)$$

for the normalized ϕ'_a and ϕ'_b , which can be written in closed forms, using the first-order approximation of, $k'_a \approx k'_b \approx k$ as

$$\phi'_a \approx \frac{V_0}{\sqrt{2}} (\sin(kx) - \sin(ky)) \quad (2.32a)$$

$$\phi'_b \approx \frac{V_0}{\sqrt{2}} (\sin(kx) + \sin(ky)) \quad (2.32b)$$

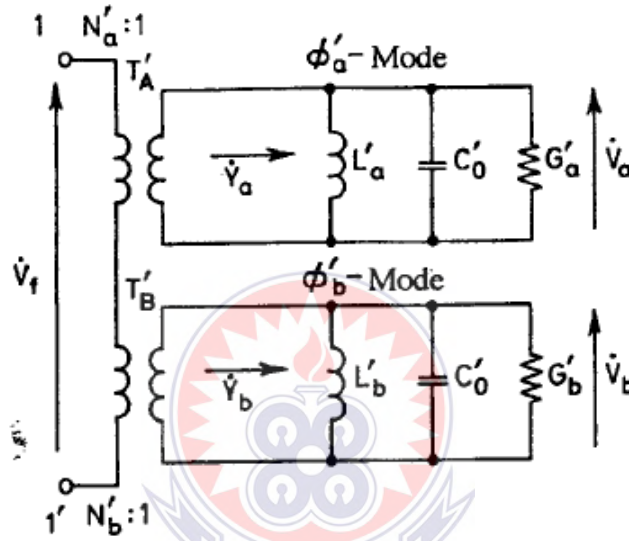


Figure 2.13 Equivalent circuit of microstrip patch antenna with perturbation (Garg, et al, 2001). It shows that the picture is picked from a paper

The energy distribution ratios for both ϕ'_a and ϕ'_b modes after perturbation are defined as turn ratios N'_a and N'_b , which are given by

$$N'_a = \frac{\sqrt{S}}{a} (\sin(kx) - \sin(ky)) \quad (2.33a)$$

$$N'_b = \frac{\sqrt{S}}{a} (\sin(kx) + \sin(ky)) \quad (2.33b)$$

Using (2.28)-(2.29b), the equivalent circuit after perturbation can be derived as shown in Figure 2.13. T'_A and T'_B represent ideal transformers with turn ratios N'_a and N'_b respectively, whereas V_f is input voltage applied to 1 – 1' terminal. \dot{Y}'_a and \dot{Y}'_b are the

patch input admittances corresponding to the orthogonally polarized ϕ'_a and ϕ'_b modes (Garg, et al, 2001). The equivalent conductance G'_a and G'_b generally include radiation, dielectric, and copper losses. However, the radiation will be the main contribution to the conductance if it is dominant as compared with the other losses (Garg, et al, 2001).

2.7.2 Type B Patch

A similar procedure used for type A can be applied to achieve different parameters for type B patch antenna, using the normalized modes ϕ_a and ϕ_b given by

$$\phi_a = V_{00}(\sin(kx) + \sin(kx)) \quad (2.34a)$$

$$\phi_b = V_{00}(-\sin(kx) + \sin(kx)) \quad (2.34b)$$

where $V_{00} = 1/a$ and $k = \pi/a$. Other parameters are given below:

$$p_1 = p_2 = \left(\frac{3}{2}\right) \left(\frac{\Delta S}{S}\right)$$

$$p_{12} = \left(\frac{-1}{2}\right) \left(\frac{\Delta S}{S}\right)$$

$$q_1 = q_2 = q_{12} = \left(\frac{1}{2}\right) \left(\frac{\Delta S}{S}\right) k^2$$

$$k'_a{}^2 = k^2 \left(1 + 2 \frac{\Delta S}{S}\right)^{-1}$$

$$k'_b{}^2 = k^2$$

$$f_a = f_{0r} + \Delta f'_a = f_{0r} \left(1 - \frac{\Delta S}{S}\right)$$

$$f_b = f_{0r} + \Delta f'_b = f_{0r}$$

$$\phi'_a = \left(\frac{\sqrt{2}}{a}\right) \left(1 - \frac{\Delta S}{2S}\right) \sin(kx)$$

$$\phi'_b = \left(\frac{\sqrt{2}}{a}\right) \left(1 - \frac{\Delta S}{2S}\right) \sin(ky)$$

$$N'_a = \sqrt{S} \phi'_a \approx \sqrt{2} \sin(kx)$$

$$N'_b = \sqrt{S}\phi'_b \approx \sqrt{2} \sin(kx) \quad (2.35)$$

Referring to the equivalent circuit in Figure 2.36, the complex amplitude ratio V_z/V_b in the orthogonal modes is given by

$$\begin{pmatrix} \dot{V}_b \\ \dot{V}_a \end{pmatrix} = \begin{pmatrix} N'_b \\ N'_a \end{pmatrix} \begin{pmatrix} Y'_a \\ Y'_b \end{pmatrix} = \begin{pmatrix} N'_b \\ N'_a \end{pmatrix} \begin{pmatrix} \frac{f_a + j(f - \frac{f_a^2}{f})}{Q_0} \\ \frac{f_b + j(f - \frac{f_b^2}{f})}{Q_0} \end{pmatrix} \quad (2.36)$$

It is assumed in (2.36), to the first-order approximation, that the unloaded Q factors Q_{0a} and Q_{0b} of the two orthogonal modes ϕ'_a and ϕ'_b are equal to Q_0 . For the patch to radiate CP, it is required that

$$\frac{V_a}{V_b} = \pm j \quad (2.37)$$

If the turns ratio N'_a and N'_b are selected such that:

$$\frac{N'_b}{N'_a} = \pm 1 \quad (2.38)$$

then (2.38) is reduced to:

$$\begin{pmatrix} \dot{V}_b \\ \dot{V}_a \end{pmatrix} = \pm \begin{pmatrix} \frac{f_a + j(f - \frac{f_a^2}{f})}{Q_0} \\ \frac{f_b + j(f - \frac{f_b^2}{f})}{Q_0} \end{pmatrix} \quad (2.39)$$

From (2.39), the frequency f and the perturbation segment $\Delta S/S$ can be found in terms of Q_0 such that the CP radiation condition (2.39) is fulfilled. This leads to the relation between $\Delta S/S$ and Q_0 , which can be expressed as

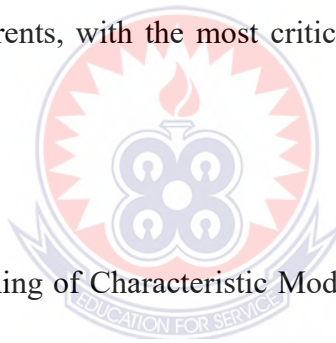
$$\frac{(Q_0^2 - 1)Q_0^2}{(2Q_0^2 - 1)} (M^2 + N^2) = MN \left\{ 1 + \frac{(2Q_0^2 - 1)MN}{M^2 + N^2} \right\} \quad (2.40)$$

Where $M = (1 + m\Delta S/S)$, $N = (1 + n\Delta S/S)$, and m and n are the constants in $f_a = f_{0r}(1 + m\Delta S/S)$ and $f_b = f_{0r}(1 + n\Delta S/S)$, which are determined from the stationary formula (Garg, et al, 2001).

2.8 Theoretical Review

2.8.1 The Theory of Characteristic Modes

The Theory of Characteristic Modes has a short yet confounded history. The idea that an item's electromagnetic properties can be depicted through a linear mix of modular field designs, not really settled exclusively by the article's shape and material composition, was initially speculated by Garbacz in 1965 (Gibson, 1979). This unique definition used a scattering matrix which is a mathematical depiction of the interaction of an object with an exciting wave. This definition gave a hypothetical verification showing that any excitable current on an item can be disintegrated in to a limitless set of radiating currents, with the most critical having the least magnitude eigenvalue (λ).



In Garbacz's dispersing meaning of Characteristic Modes (CMs), every eigenvalue is characterized as far as the radiation obstruction of the relating current. Be that as it may, this hypothetical prologue to CMs needed earlier information on trademark far-field radiation designs and their related eigenvalues. In this work Garbacz gave two potential answers for tracking down the obscure modes; the two techniques are hard to carry out and impractical to use on all item calculations.

With this critical downside there was no published investigation into this theme for an additional six years. In May 1971, Garbacz again presented the subject of scattering-

based theory of Characteristic modes (TCM) to the scholarly community. In Chen and Chia (2006), an unmistakable definition to TCM is expressed to be " At a given frequency every perfectly conducting obstacle has associated with it a particular set of surface currents and corresponding radiated fields which are characteristic of the obstacle shape and independent of any specific excitation." This overall definition to TCM has since stayed with just a single minor change, that TCM is presently not related with just Perfect Electric Conductors (PEC) (Wang and Du, 2015).

2.8.2 Antenna Synthesis

Antennas Synthesis Antennas are commonly synthesized through a difficult improvement technique, where the feeding structure, feed area, and item are totally changed with an end goal to acquire the best antenna performance. Albeit an antennas's radiation performance is on a very basic level restricted by its shape and material, common investigation instruments are not appropriate for this sort of improvement as there is the requirement for feeding structures. Notwithstanding, TCM is impeccably appropriate for antenna synthesis algorithms as it just breaks down the presentation of the article and doesn't need any excitation structures (Chen and Chia, 2003). Furthermore, TCM-based calculations can be created to integrate or streamline an object and anticipate the best areas to execute excitation structures (Chiu et al, 2012). After an article is enhanced, other computational investigation instruments can be used to combine and upgrade feeding structures in the areas already determined by TCM examination.

2.8.3 Performance Requirement of Slot Antennas

Antennas are fundamentally described by specific parameters which are for the most part dependent on the application for which the antenna is planned. In this segment, a short analysis of the required performance of the proposed broadband slot antenna in this study, in view of the above parameters is provided.

2.9 Empirical Review of Slot Antenna Design and its application

Kerketta (2012) designed a wideband printed slot antenna suitable for wireless local area network (WLAN) and satisfying the worldwide interoperability for microwave access (WiMAX) applications. The antenna was a microstrip line fed antenna with a fractal geometric structure that used iteration techniques to lower the antenna's resonant frequency. The project's goal is to discover the radiation pattern and return loss. Analysis of fractal antenna was done by using Software named CST Microwave Studio Suite. The antenna size inclusive of the ground plane was compact and had a wide operating bandwidth. The antenna exhibited omnidirectional direction radiation coverage with a gain better than 2.0 dBi in the entire operating band.

The study found that CPW-fed Koch fractal printed slot antenna is suitable for WLAN 2.4/5.2/5.5 GHz and WiMAX 2.5/3.5/5.5 GHz operations. This geometry lowers the frequency of operation along with wide band matching and antenna size is compact as well as simple. The study also established that Perturbed Sierpinski carpet fractal antenna with CPW feed is suitable for WLAN applications. The overall size can be

effectively utilized for integrating with other components in WLAN communication devices.

Broadband planar antennas with a wide rectangular slot and multiple tuning stubs were examined by Saed (2006). Coplanar waveguides feed the antennas. Wide slots with a single tuning stub, V-shaped stubs, and inverted F-shaped stubs are all being studied. Despite using a substrate with a high dielectric constant, the antennas had a wide bandwidth. The antennas also had broadside bidirectional radiation, according to the study. For the various setups, the radiation pattern stability with frequency was given. The inverted F stub in a broad rectangular slot, one of the proposed configurations, exhibited exceptionally steady radiation patterns over its whole impedance bandwidth of around 40%. The V-shaped stub in a rectangular slot also achieved a 44 percent impedance bandwidth.

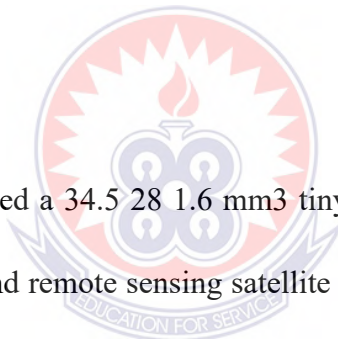
Jen-Yea and Liang-Chin (2009) designed a printed microstrip-line-fed rhombus slot antenna with a pair of parasitic strips. The study established that with the use of these parasitic elements along the microstrip feed line, bandwidth enhancement for wideband operation can be obtained. From experimental results, the measured impedance bandwidth, with a 10 dB return loss, can operate from 1.80 to 6.09 GHz which is wider than a conventional microstrip-line-fed printed rhombus slot antenna without parasitic elements. The proposed antenna may enable PCS, IMT-2000, and

WiMAX multiband operations for various wireless communication services by selecting correct parasitic strip dimensions.

A broadband planar antenna with consistent radiation patterns was designed by Xianming (2008). It consisted of a hanging radiator that was fed vertically by an n-shaped microstrip. With a return loss of $|S_{11}|$ -10 dB and an average gain of 7.7 dBi, the measured impedance bandwidth was 3.1–5.1 GHz. There was no evidence of beam squinting across the operating frequency band. It was also a cost-effective design with good mechanical tolerance and manufacturability.

Li et al (2007) designed a compact broadband planar antenna for global positioning system (GPS), DCS-1800, IMT-2000, and WLAN handsets. An S-strip and a T-strip were printed separately on the two sides of a thin substrate to make the planar antenna (no via process was involved in the fabrication). The antenna was just 18 mm long, 7.2 mm wide, and 0.254 mm thick, making it smaller than previously documented antenna layouts. The mutual interaction between the S-strip and the T-strip increases the planar antenna's bandwidth. Simulation and testing have shown that the small planar antenna may achieve a bandwidth of more than 50% for a return loss of 10 dB while maintaining a nearly same radiation pattern.

A printed microstrip-line-fed antenna featuring a broad rotating square slot, a rotated patch, and a pair of tuning stubs was designed by Oteng and Guangjun (2002). The bandwidth augmentation for broadband operation was achieved by adding a pair of tuning stubs to the feedline and introducing an additional resonance in the high frequency range. The antenna can operate with a reflection coefficient of less than -10 dB from 2.38 to 9.64 GHz, according to measurements. This was found to be almost twice the bandwidth achieved by the microstrip-line-fed rotated slot antenna without the tuning stubs. The study indicates that by choosing the right tuning stub dimensions, the antenna can be used for a variety of wireless applications requiring wideband and multiband operation.



Sharma et al. (2020) developed a 34.5 × 28 × 1.6 mm³ tiny antipodal structured antenna for broadband applications and remote sensing satellite communications. The antenna design included an antipodal radiator and a faulty ground plane. For improved bandwidth, good impedance matching, and to prevent connecting pins for the top and lower halves of the antipodal radiator, the design structure was supplied via a balanced tapered microstrip feed-line. Mathematical calculations were proposed for the dominant mode frequency.

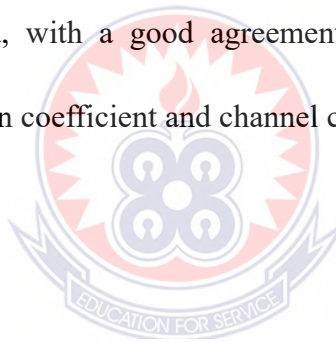
Their study optimised antenna parameters using commercial simulator before fabrication and validation of antenna prototype using FR4 epoxy dielectric substrate.

The result of the study was consistent with simulated results from 5 GHz to 40 GHz. The simulated and measured results of return loss, beam-width, far field pattern, and group delay were employed to evaluate the performance of the antenna. Further, antenna performance was also found satisfactory in deployable application device and several plastic housings.

Cui and Fu (2014) designed a broadband dual-polarized planar antenna for 2G/3G/LTE base stations. Two perpendicularly crossed bow-tie dipoles made up the dual-polarized antenna. The dual-polarized antenna is fully planar since each bow-tie dipole is driven by a microstrip stub that is directly supplied by a coaxial cable. A large bandwidth was attained thanks to the connection of two crossed bow-tie dipoles. The study shows that the dual-polarized antenna has a bandwidth of 45% (1.7-2.7 GHz) for return loss >15 dB with an isolation of higher than 30 dB between two polarization input ports. The dual-polarized antenna has a half-power beam width (HPBW) of around 65° and an average gain of 8.5 dBi for slant $\pm 45^\circ$ polarizations. An 8-element dual-polarized planar antenna array was developed for base station applications. The antenna array achieves a bandwidth of 56 percent (1.63-2.9 GHz). The array's antenna gain is around 16 dBi, and the HPBW for each polarization is 658 degrees.

Hiraga (2013) designed and analysed printed crescent shape monopole antenna,

Planar Inverted F-L Antenna (PIFLA) and Planar Inverted FF Antenna (PIFFA). The antennas exhibit broadside directional pattern. The performances such as return loss, radiation pattern and current distribution of the UWB antennas were found satisfactory (under - 10dB point in the bandwidth of UWB) using simulation. The study also investigates into the miniaturization of MIMO/diversity Planar Inverted-F antenna (PIFA) which is suitable for pattern diversity in UWB applications. This antenna assembly is formed by two identical PIFAs, a T-shaped decoupling structure which connects the two PIFAs and a finite ground plane with a total compact envelope dimension of 50 x 90 x 7.5mm³. The MIMO antenna's radiation performance was very good, with a good agreement between the computed and measured envelope correlation coefficient and channel capacity loss.



CHAPTER THREE

METHODOLOGY

3.1 Conceptual Methodology

The design of the broadband planar slot antenna will be based on the procedure given by Luxey (2004). This can be used as a starting point for sizing. An electromagnetic simulator can then be used to carry out the optimization. With a typical impedance of 50, the antenna is stimulated. The design will employ slot approaches, with gain and directivity taken into account. The slot's aim will be to control the radiation pattern in order to enhance bandwidth. The optimization of theoretical parameters design will be done by using Finite Element method software integrated into High Frequency Simulation Software version 19 (HFSS 19), which contains different techniques and calculation methods. After many optimizations and miniaturizations, the dimensions and performance properties of the final optimized design structure will be listed and compared to currently existing slot antennas to show its novelty.

The objective of this work is to come up with a compact slot antenna that offers an improved bandwidth to cover the entire IEEE C-band, hence, the bidirectional pattern will be maintained for the proposed design.

3.2 Design Methodology Using HFSS Software

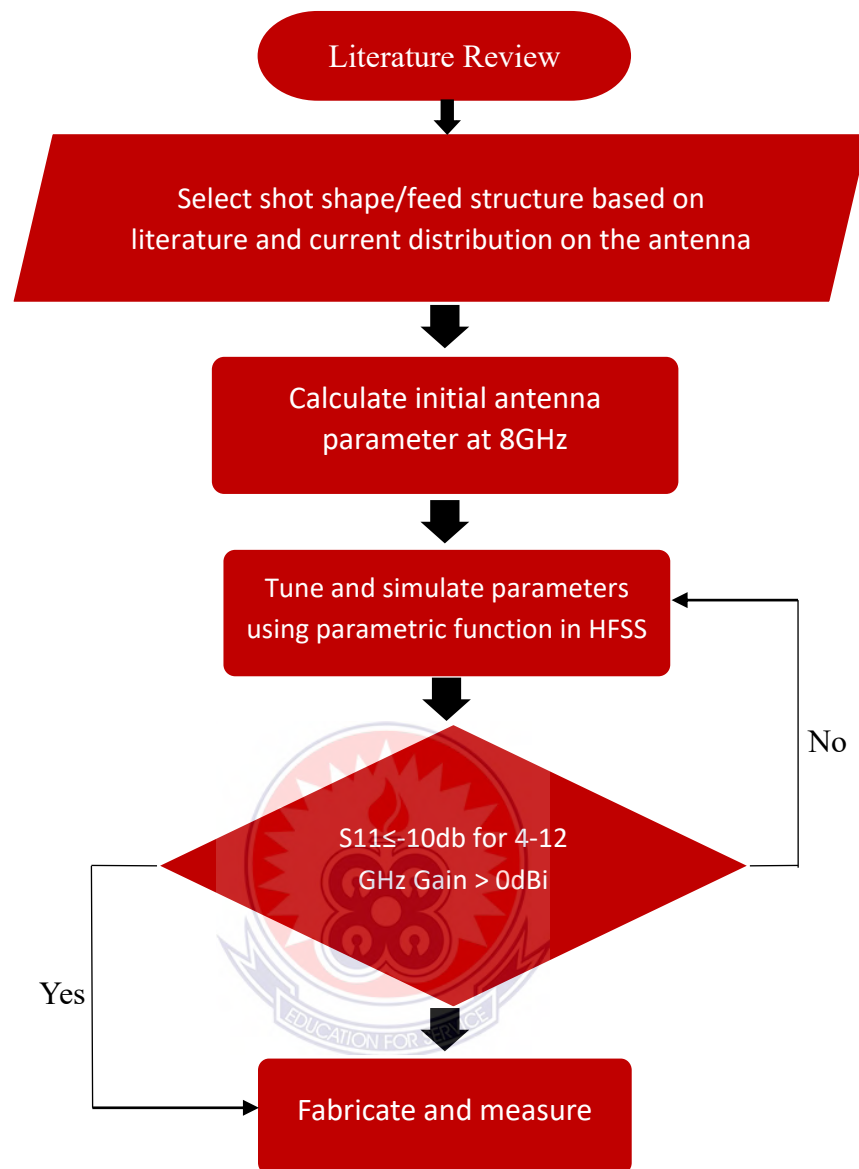


Fig. 3.1 Antenna design Flow chart

Design methodology using the HFSS software is depicted in fig 3.1, which primarily involves the development of a broadband antenna from an initial simple square slot design. The HFSS software is based on the finite element method (FEM) for solving electromagnetic field problems. In the software, users create electromagnetic structures based on their initial theories and the software analyzes the structures to

generate desired results.

In the next section, the design procedure using the HFSS 19 software is discussed.

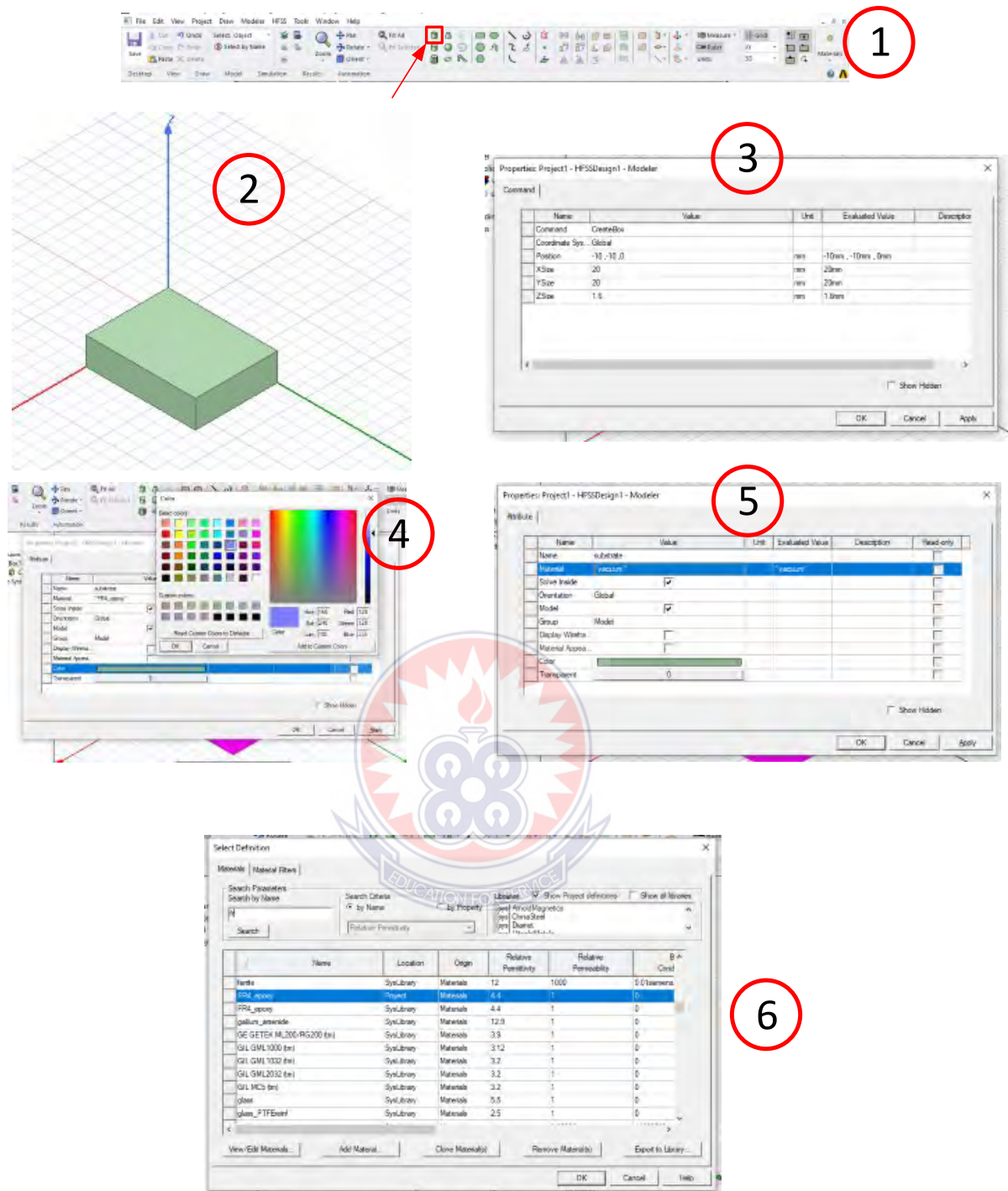
3.3 Antenna Design Procedures

The design procedure is broken down into a number of steps which are elaborated on in this section. In fig 3.2 these are provided for easy replication of the proposed antenna in HFSS. The following were considered such as the radiator, the stab, microstrip and excitation port

3.3.1 Substrate

A slot antenna is a planar antenna that is printed on a dielectric substrate. The first step in the design process is to select the dielectric substrate. FR4 epoxy with a dielectric constant of 4.4 and a height of 1.6 mm is chosen due to its low cost and ease of availability should the antenna be fabricated.

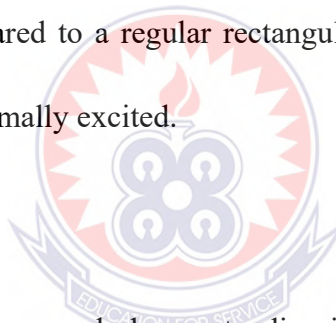
Draw arbitrary box and set dimensions (i.e. substrate area and height)



3.3.2. Radiator

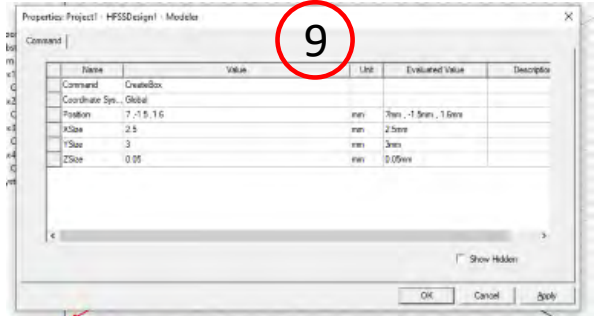
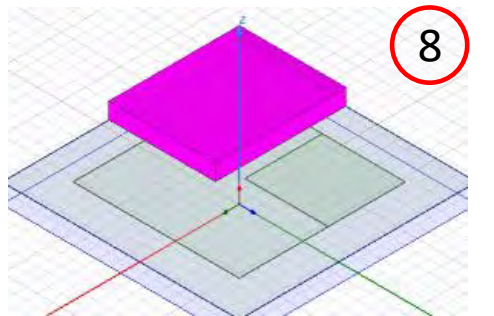
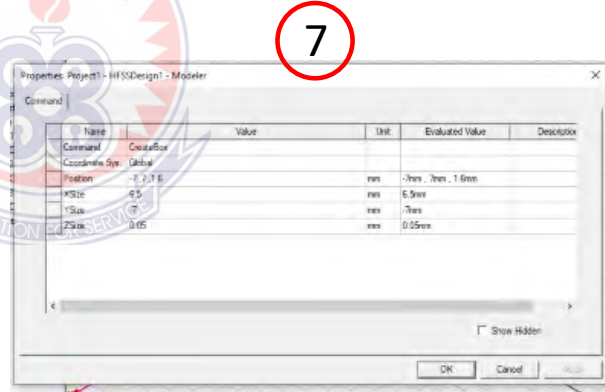
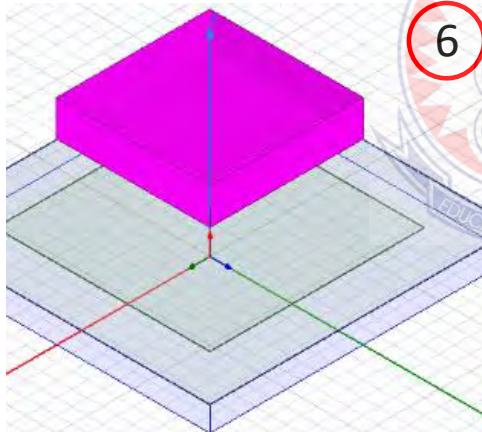
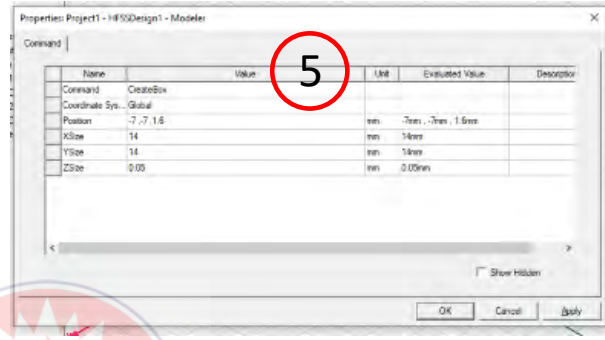
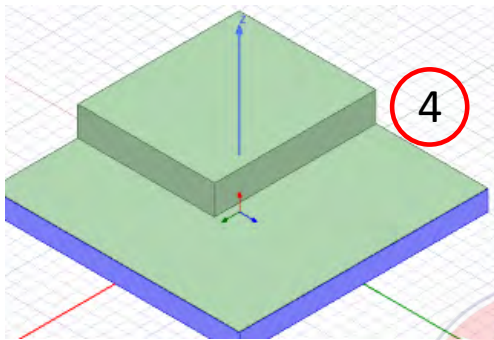
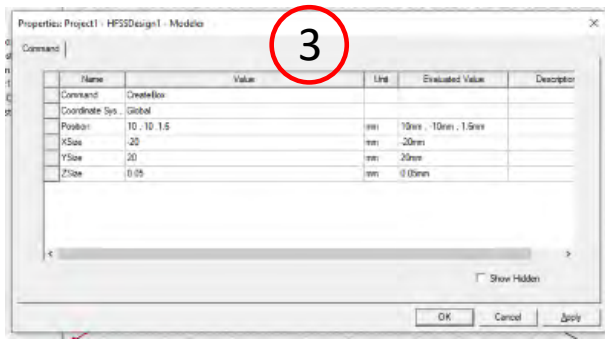
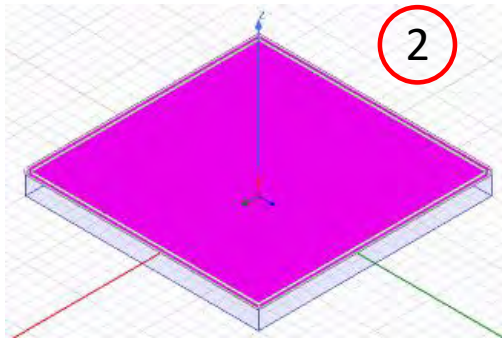
The next step is to design the radiator on the substrate. A slot antenna's radiator is basically a slot etched in the ground plane which is a conductor. In this design, the conductor chosen for the ground plane is copper. Aluminum could have been used as

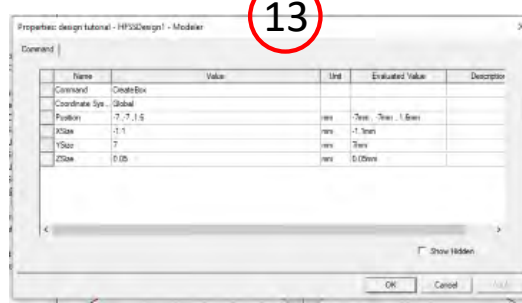
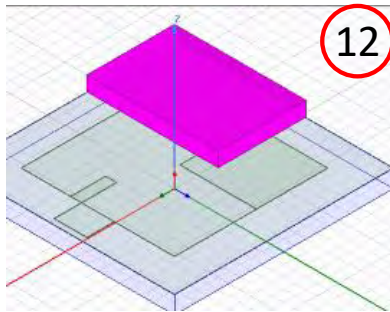
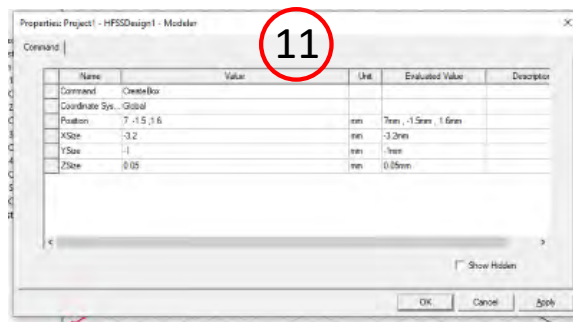
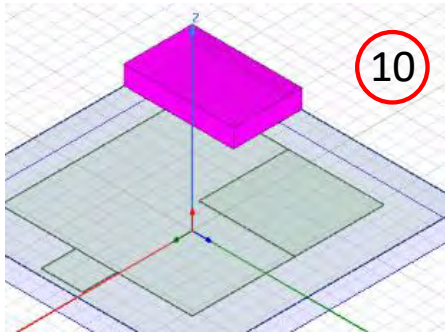
well without it affecting the desired results. These two conductors are mostly used again as a result of their low cost. In the simulation, a perfect electric conductor (PEC) could have been employed as the conductor, however, boxes instead of sheets were used for the design of all conductors, thus leading to the choice of copper over PEC. The ground plane area is chosen to be the same as the substrate area. The height of the ground plane is chosen to be 0.035 mm which is the standard thickness of conductors used for fabrication of microstrip antennas (Balanis 2014). The shape of the slot which is the main radiator is then etched into the copper by subtraction in the software as shown in the. The L shape was chosen because it provides a longer path for the current distribution as compared to a regular rectangular or square slot leading to a broader bandwidth when optimally excited.



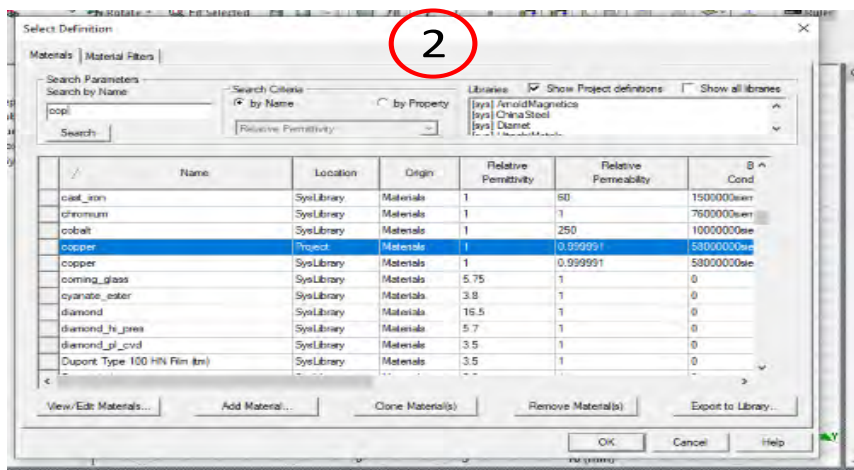
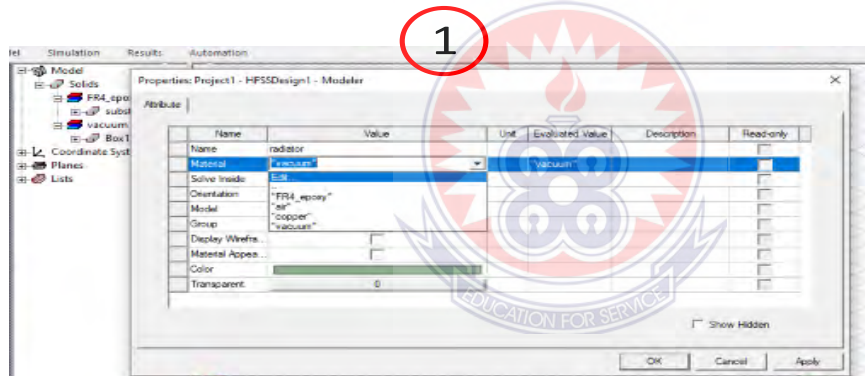
3.3.3 A Stab

A stub is then attached to the ground plane extending into the slot radiator to further increase the current path. This is done by simply uniting the stub with the ground plane using the "unite" feature in the software. The stub is also a conductor and thus has the same height as the ground plane. The length of this stub is chosen based on a parametric study in HFSS which will be discussed in detail subsequently.

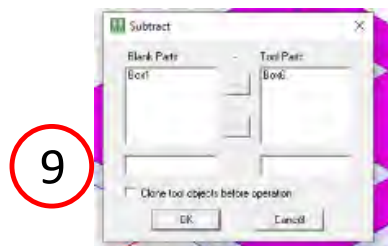
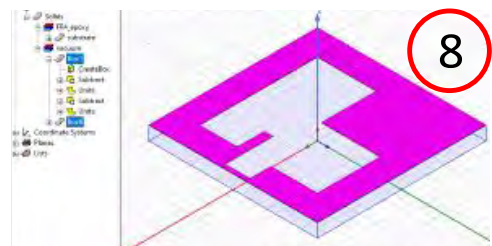
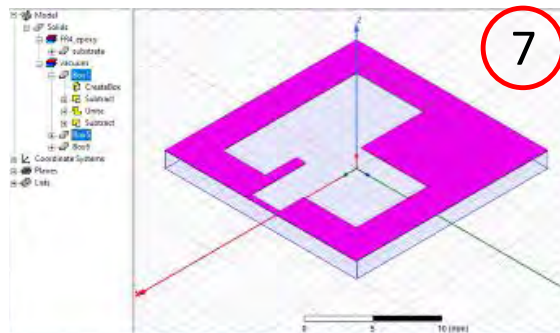
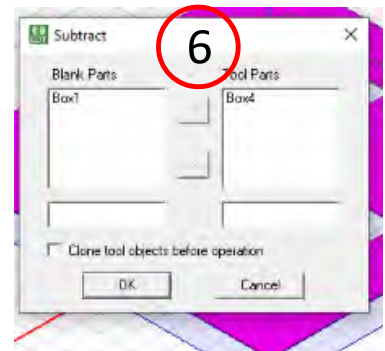
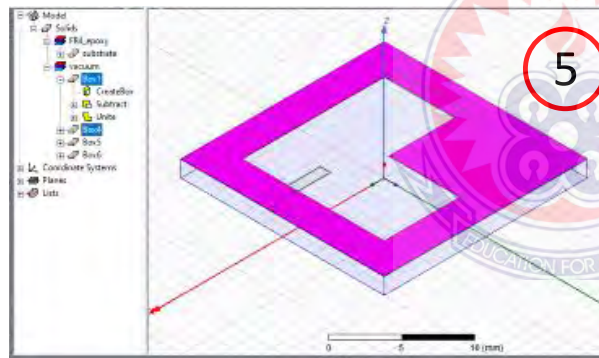
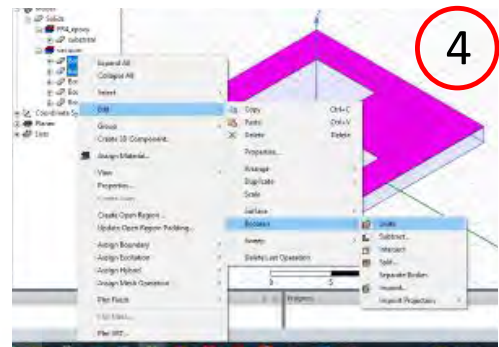
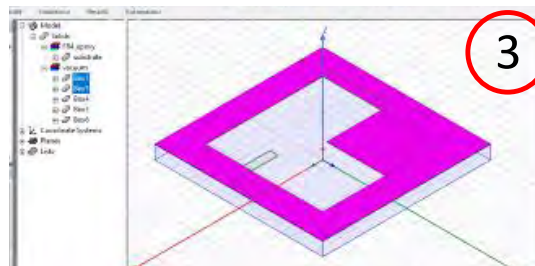
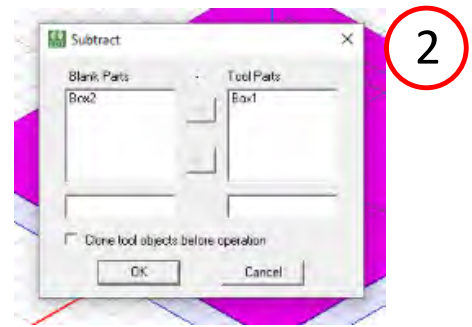
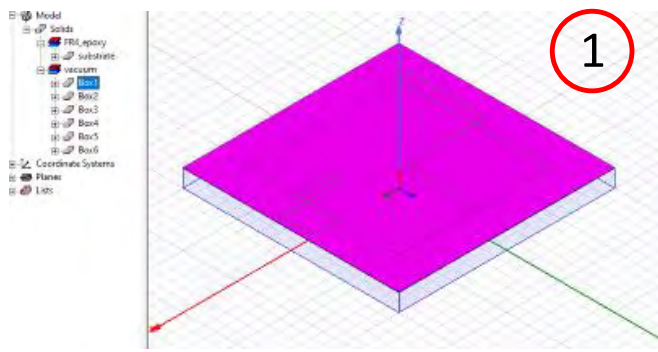




Assign Material (box1) copper



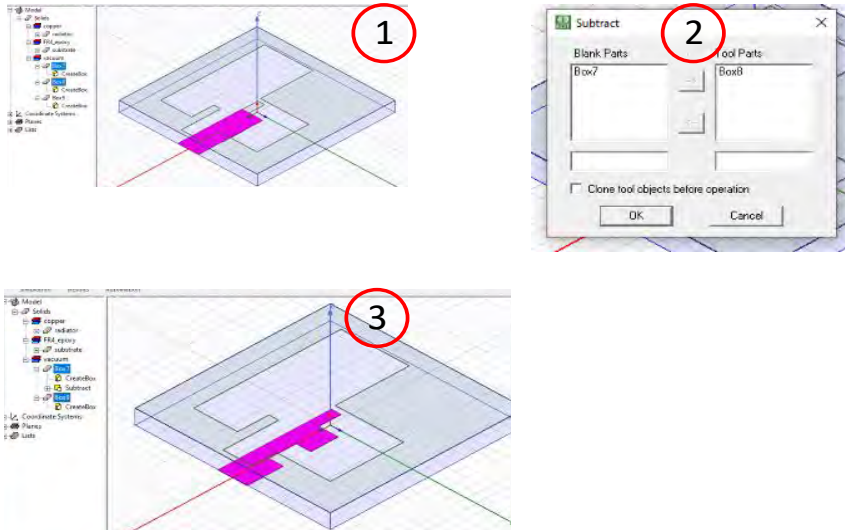
Unite and Subtract elements



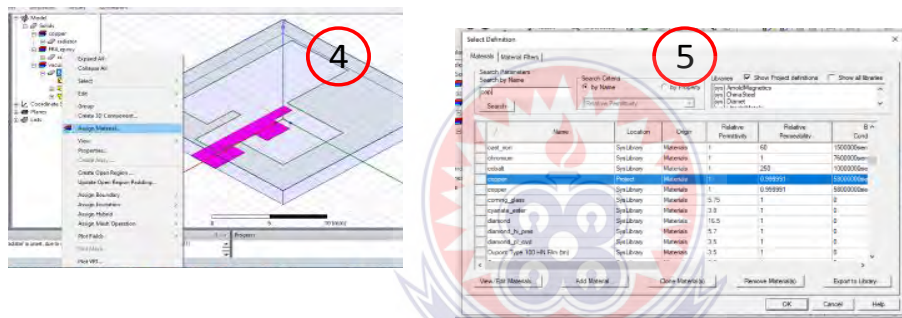
The next step is to design the microstrip feedline which will feed the slot radiator with the electromagnetic energy. The dimensions for this feedline can be arrived at using equations from chapter 2 or by using a microstrip patch calculator which is accessible online. After achieving the dimensions from the calculator, a slot and stub are etched on the feedline to enable optimum coupling between it and the slot radiator leading to a broad band antenna. The stub and slot combination have been employed for different purposes including generation of circularly polarized waves in microstrip antennas. The effects of this stub and slot on the antenna performance will also be discussed in chapter 4.



Unite and subtract elements

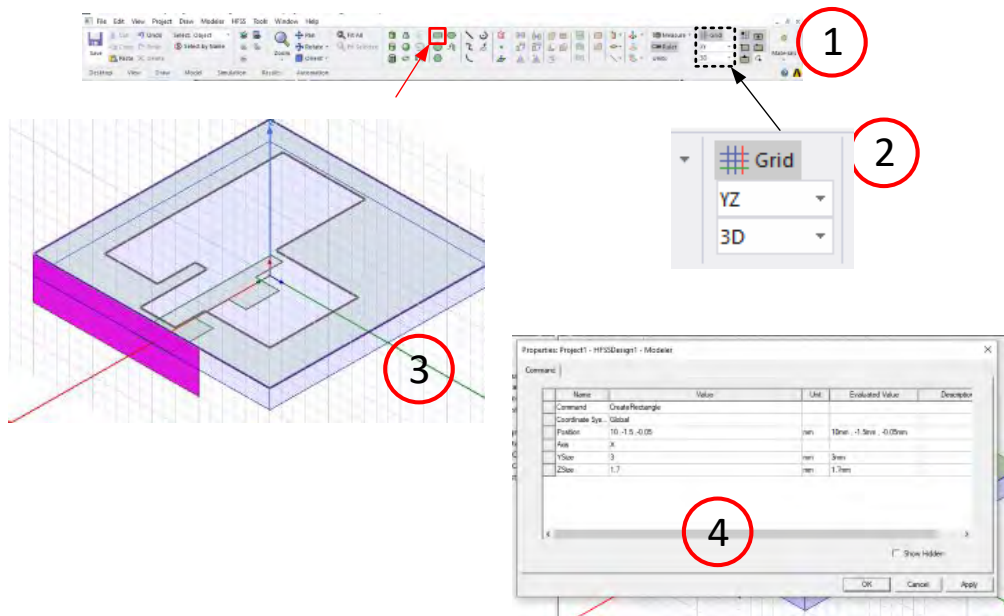


Assign Material (box7) copper

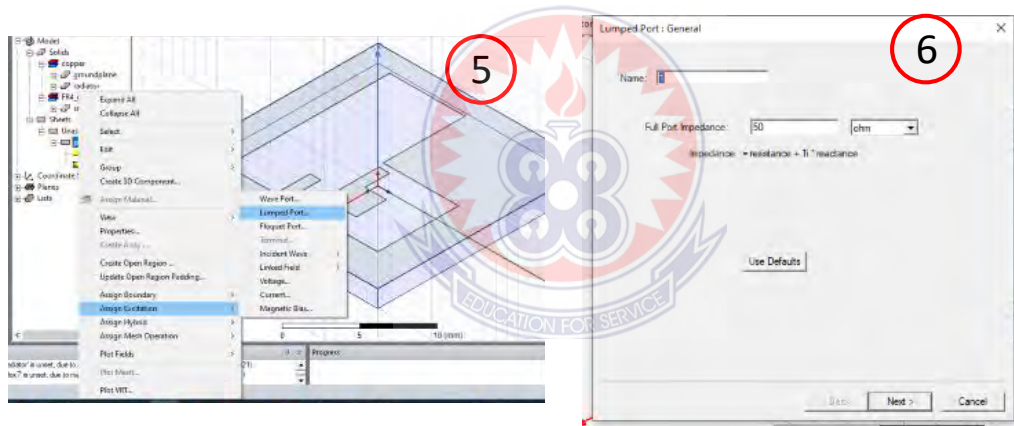


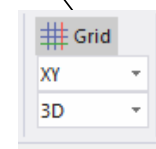
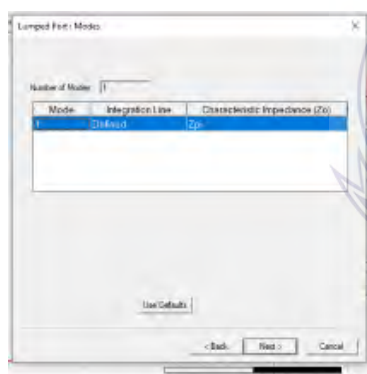
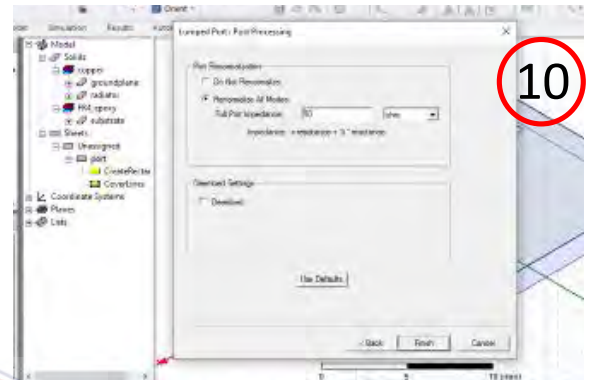
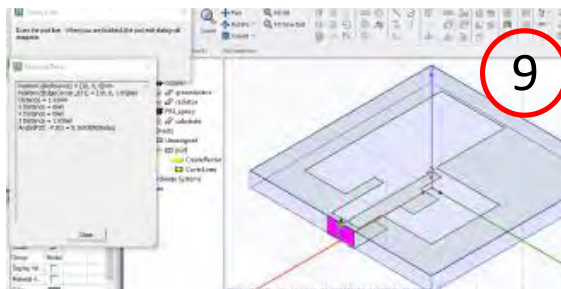
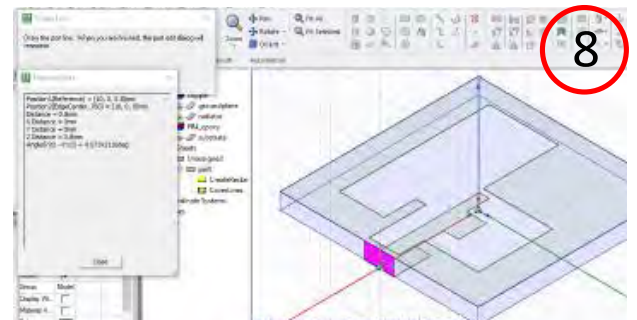
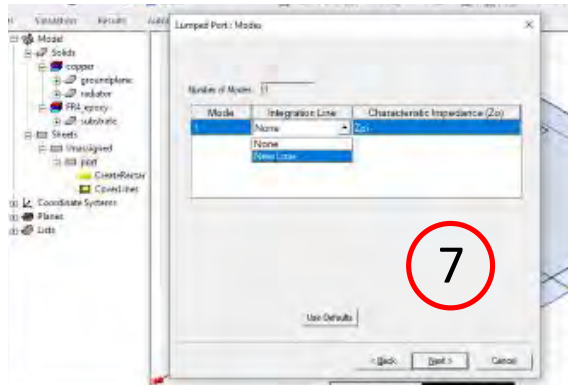
The next step in the design process is to add an excitation port to the feedline to serve as the power source. There are number of ways of achieving this in HFSS (i.e. using a wave-port, Floquet port or a lumped port). In this design, a lumped port is preferred as there are metals on both sides of the substrate. An impedance of 50 ohms is chosen for the port and the design of the feedline as it is the most widely used for wireless devices.

Port



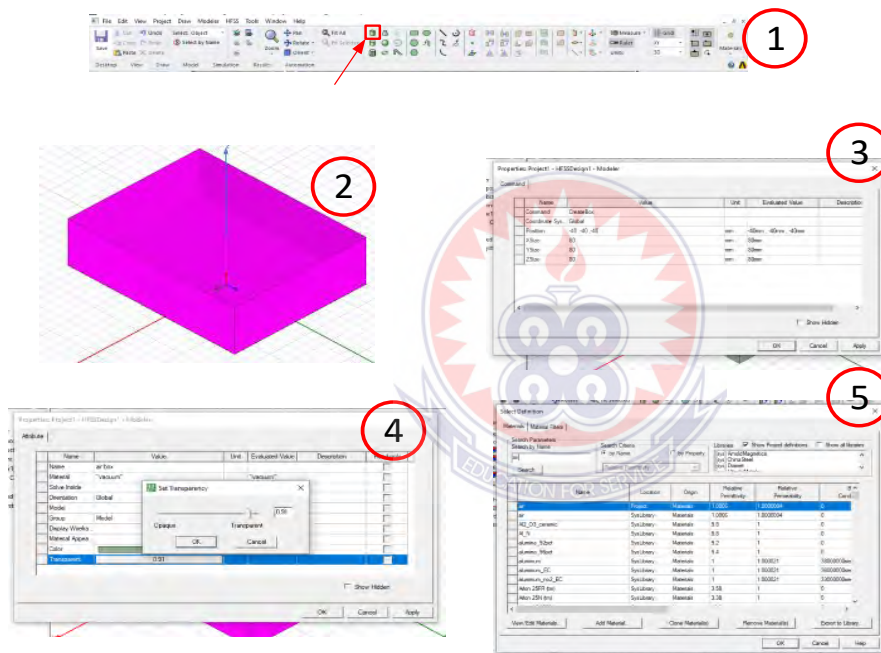
Port Assignment



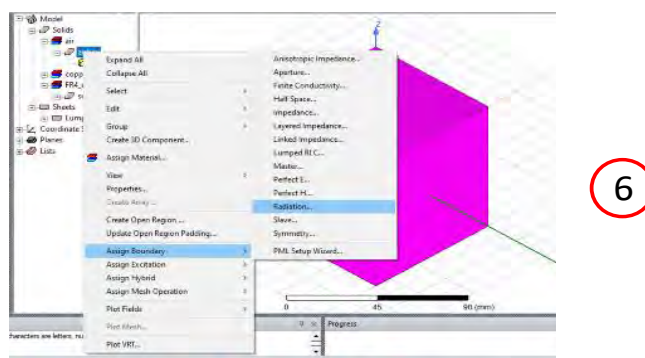


The next step in the design process is the introduction of a radiation box to mimic an anechoic chamber. When antennas are fabricated, they are first tested in an anechoic

chamber to ensure they work optimally before being deployed. In HFSS this is achieved by drawing a box around the designed antenna with the sides of the antenna being a distance of at least half wavelength away from the insides of the box. This is done to ensure that the antenna radiation that is tested is in the far field of the antenna. The designed box is assigned a radiation boundary to mimic the foam materials that are found in anechoic chambers. Their purpose is to ensure that all radiations are confined to the insides of the anechoic chamber (radiation box in the case of HFSS).



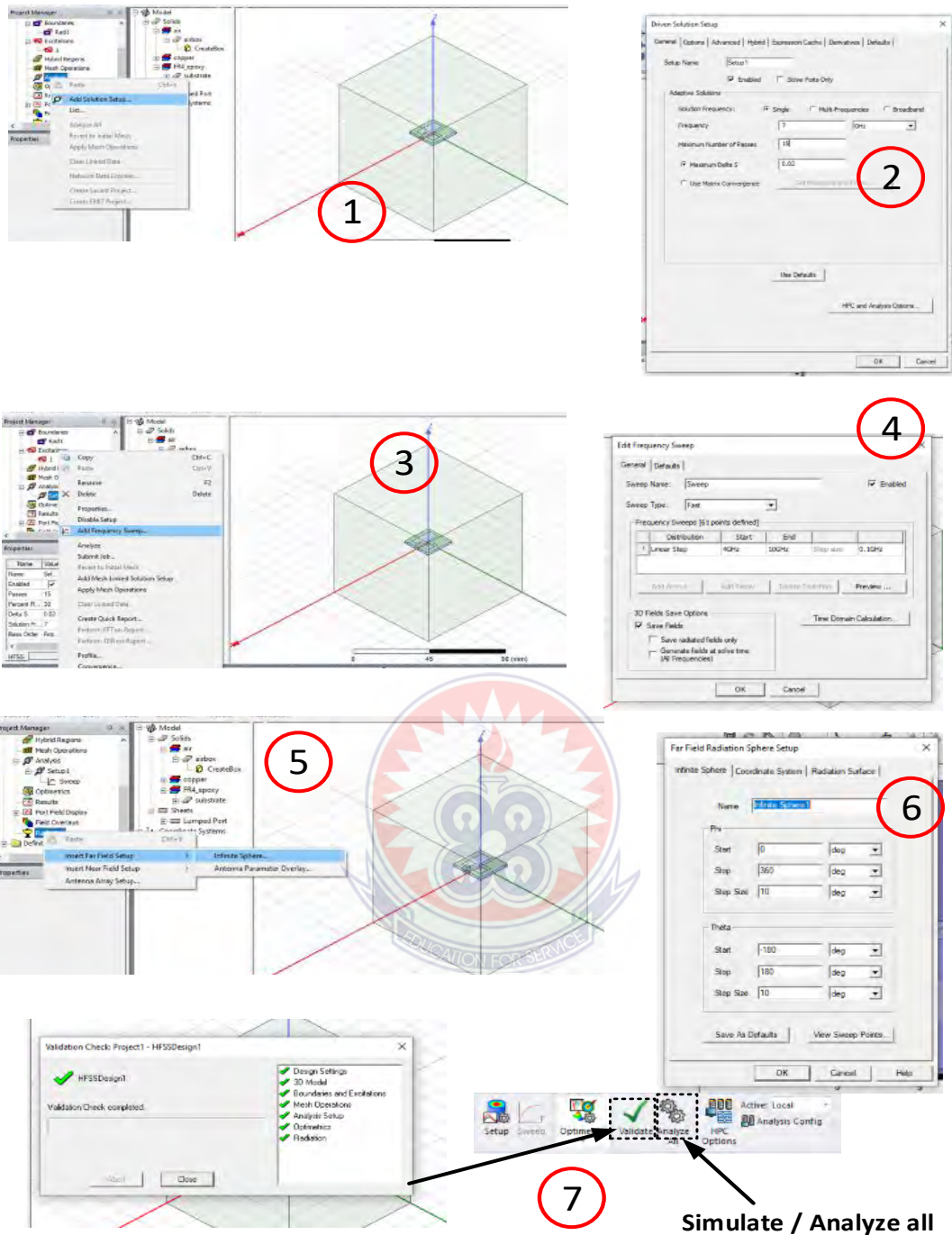
Assign Radiation Boundary



3.4 Simulation Parameters and Processes

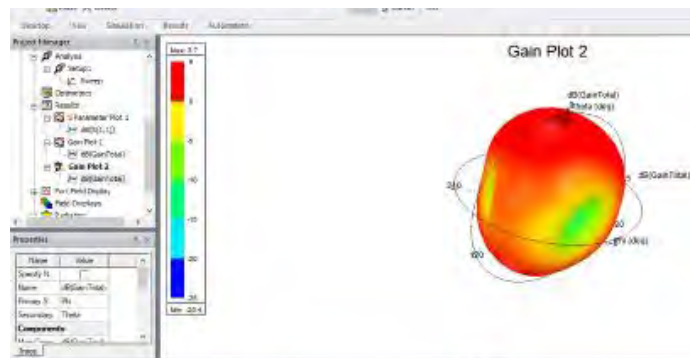
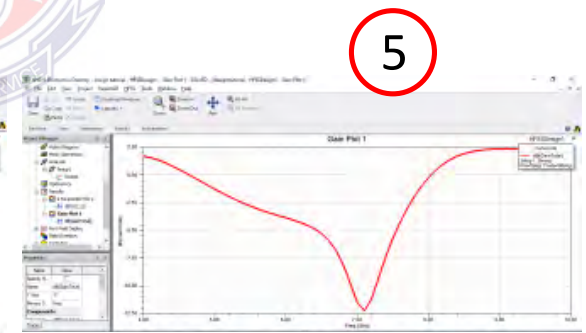
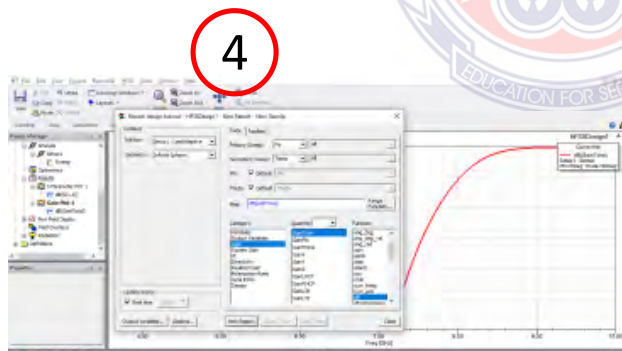
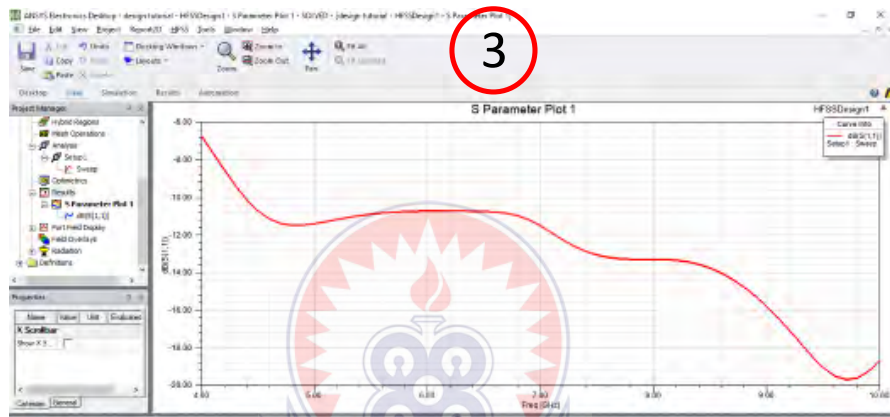
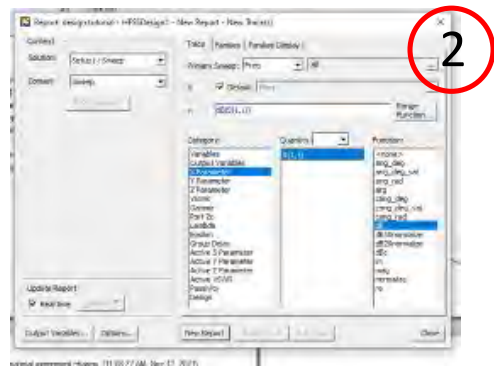
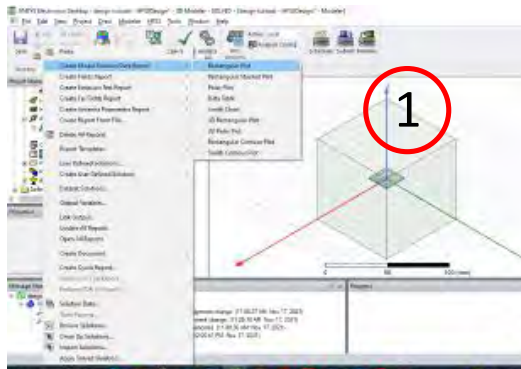
In this work, frequency interval of 4 - 13 GHz with a center frequency of 8.5 GHz is used. A step size of 0.1 GHz is chosen for smooth curves and more accurate results. The type of simulation used is "Fast" because of the low specifications (specs) of the computer used for the simulation in addition to wanting a quick but accurate simulation. Interpolation could have been used looking at the wide frequency range, however, it would not have given very accurate results. Discreet would have taken a longer time and provided even more accurate result but could not run on this computer due to low specs.

An infinite sphere is also added to mimic the spherical coordinate system which is used for the radiation pattern plots. Theta and Phi angles ranging between 0 - 180 degrees and 0 - 360 degrees respectively are used with a step size of 10 degrees each. After inputting all the data mentioned above, the simulation setup is validated to ensure there are no errors and the simulation is run.



When HFSS finishes its run, the results can then be generated by clicking on the results tab and generating the desired results which in this case are the S_{11} , gain and radiation patterns at specific angles.

Results



It is worth mentioning that the 3D radiation patterns are not plotted as the proposed antenna is broadband and hence having patterns at just one frequency point to depict the gain there would not provide any useful information for antenna engineers as compared to having a 2D plot to show the gain response over the entire frequency range.



CHAPTER FOUR

ANTENNA SIMULATION RESULTS AND DISCUSSION

This chapter presents and discusses the various results of the simulation

4.1 L Slot Antenna Configuration

The geometry of the proposed antenna is as shown in Figure 4-1. The proposed antenna has the basic configuration of a microstrip slot antenna. In this design, the center frequency of the antenna is chosen as $f_c = 8$ GHz ($\lambda = 37.5$ mm, where, λ is the wavelength at 8 GHz). The wavelength is calculated by using the formula and half of the value obtained ($37.5/2$ mm) is used as the starting dimension of the designed antenna which is then optimized in the simulation tool to arrive at the dimension shown in Table 4.1.

$$c = f \lambda$$

Where, c = the speed of light (3×10^8 m/s), f = frequency

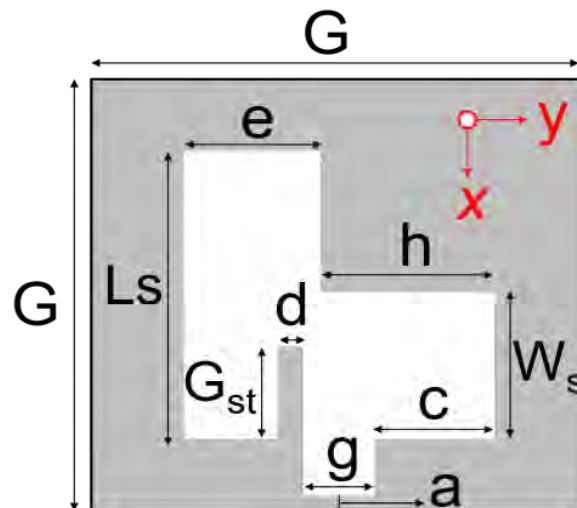


Fig 4.1 (a)

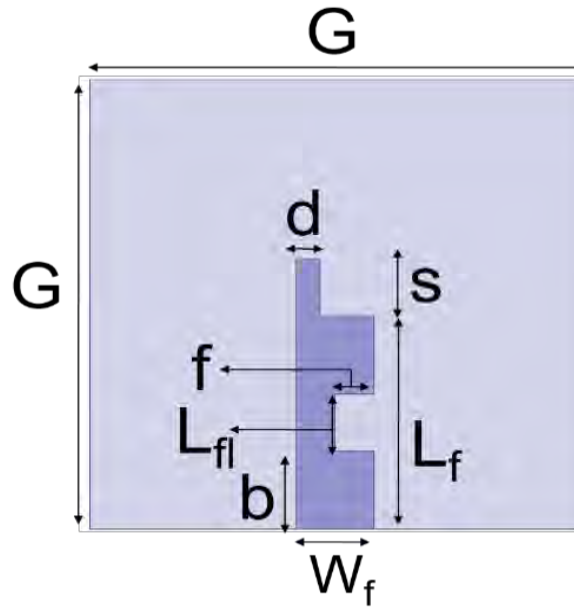


Fig 4.1 (b)

Figure 4- 1 Geometry of the Proposed Antenna. (a) Top side (b) Bottom side

The antenna is composed of an L-shaped slot etched in the ground plane made of copper, a stub attached to the ground plane with a rectangular slot as well to aid in effective coupling between the feedline which is etched on the opposite side of the ground plane on the same dielectric substrate and the radiating L-slot. The feedline has a slot etched in its midpoint and has a stub attached to it as shown in Fig 4b. The ground plane with the slot and microstrip feedline are all etched on an FR4-epoxy dielectric substrate with a thickness of $h = 1.6\text{mm}$ and relative permittivity (ϵ_r) of 4.4. The antenna has a ground plane size of G . The radiating L slot is designed by first subtracting the vertical side with dimensions $(L_s * e)$ from the copper on the ground plane and then subtracting the horizontal portion with dimension $(W_s * h)$ as well. A slot with a size of $(b * g)$ is etched in the lower side of the ground plane as shown in

The feed-line which is placed on the opposite side (referred to as the bottom side) of the substrate has a width (W_f) which was chosen to match the 50Ω port impedance to ensure good impedance matching. The length of the feed-line was also chosen to be L_f so as to achieve a good matching performance. Table 4.1 shows the optimized dimensions of the proposed antenna.

Table 4- 1 Antenna Parameters

PARAMETER	SIZE (mm)
G	20
W_s	7.5
L_s	15.1
W_f	3
G_{st}	3.2
D	1
L_{fl}	2.8
L_f	9.3
E	7
H	7
C	5.5
G	3
A	0.5
S	2.3
F	1.5
B	3.7

The evolution of the design process of the antenna is shown in Fig 4.2. This is done to show the working principle of the antenna. A basic slot antenna is first designed at a frequency of 8 GHz as already mentioned. As observed from Fig 4.3, this antenna named Antenna I possesses a wide impedance bandwidth that covers almost the entire IEEE C-band. This is because the slot antenna in its basic form is known to operate as a wideband antenna. Antenna II consists of an L-slot and a rectangular slot at the bottom of the ground plane. A wider impedance bandwidth is achieved as a result of the effective coupling between the feedline and the L-slot. This is aided by the rectangular slot at the bottom of the ground plane which acts as a quasi CPW slot. In Antenna III, stubs are placed on the ground plane and feedline. This technique was employed by Zhang et al to improve the ground plane by breaking the surface current distributions on it for the generation of circularly polarized waves. When this is done, the reflection coefficient is observed to shift into the higher frequency range and deteriorate around 7.7 - 8 GHz. A slot is therefore etched into the lower section of the feedline to enhance the reflection coefficient.

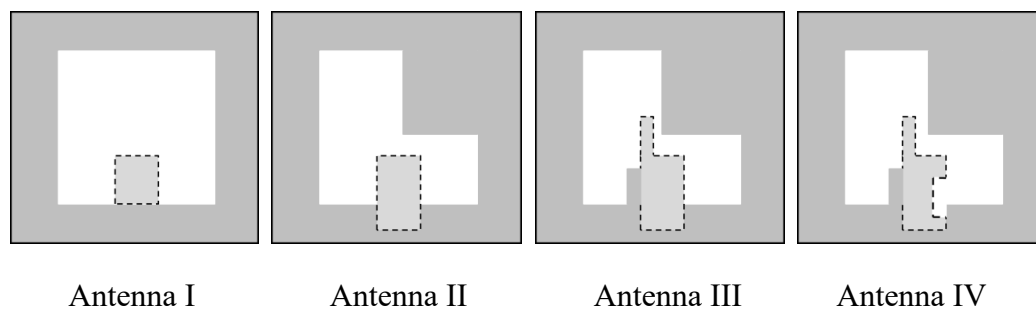


Figure 4.2 Evolution of antenna design

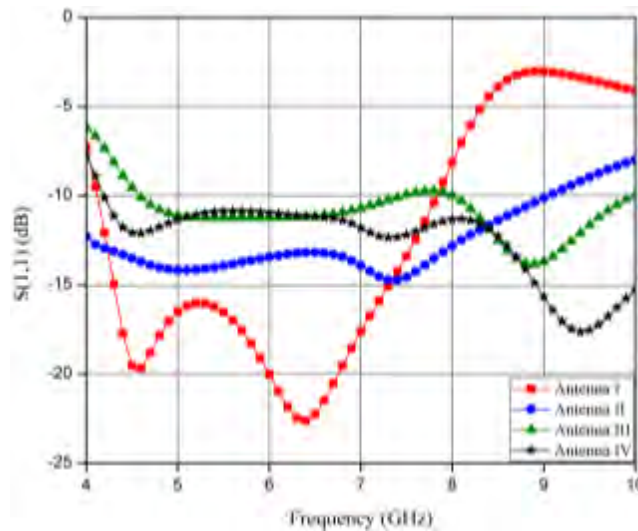


Figure 4.3 Reflection coefficient of antennas I-IV

4.2 Parametric Study

A parametric study is done to show the effect that the various parameters of the antenna have on the reflection coefficient. This is done to provide a useful guideline for practical design applications as well as to show the thinking behind the choice of the dimensions. It is worth mentioning that, when one parameter is studied, all others keep their optimized values as given in Table 4.1.

A. The Effect of the Ground stub length (Gst)

Fig 4.4 illustrates the effect of the length of the ground plane stub (Gst) on the reflection coefficient. The stub with five different lengths is studied while other parameters remain fixed. As seen from Fig 4.4, the stub length has a direct effect on the S11 in the mid frequency range. It is observed that the S11 deteriorates starting from the mid frequency range as the length is either increased or decreased with

respect to the optimum value of 3 mm. Thus, a value of 3 mm is chosen for this parameter.

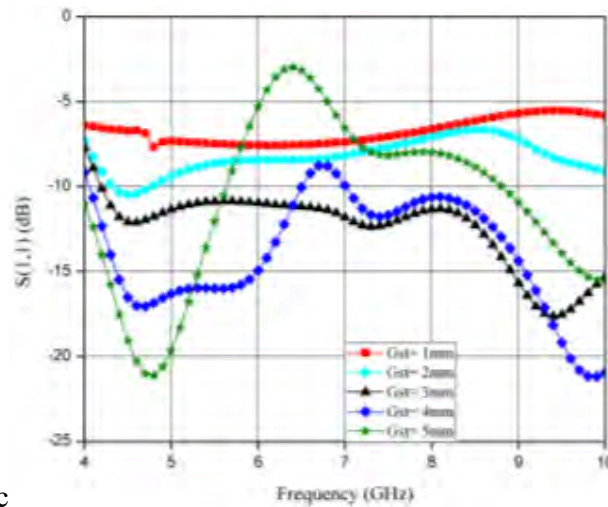


Fig 4.4 Reflec

tion coefficient for antenna IV with different lengths of ground stub (Gst)

B. The Effect of the Feedline Stub length (s)

The effect of the length of the feedline stub (s) on the reflection coefficient is also studied in Fig 4.5. It is realized that this parameter has great effect on the impedance bandwidth in the lower frequency range. As the length is increased from 1mm to 5mm with all other parameters keeping their optimized values, it is observed from Fig 4.5 that the S11 in the lower frequency range deteriorates. However, a length of 3 mm gives the most optimum results.

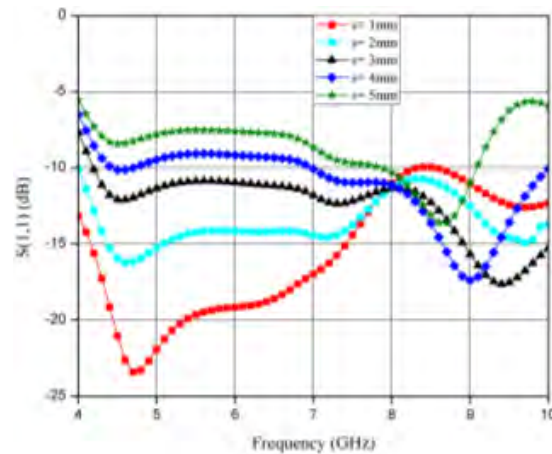


Fig 4.5 Reflection coefficient for antenna IV with different lengths of feedline stub (s)
4.3 L Slot Antenna Performance Simulation

Simulated results of the proposed antenna are as shown in Figures 4-6 (a) and (b). It is seen from Fig. 4-6a that the simulated reflection coefficient is less than -10dB over the frequency ranges of 4.2 – 12.8 GHz which covers the entire IEEE C-Band and X-Band. This is mainly due to the effective coupling of the EM waves from the feedline to the wide slot which is made possible by the slot shape and stubs attached to both the feedline and the ground plane. Fig. 4-6b shows the simulated gain. The results show that the antenna has a gain above 2.5dB in almost the entire operating frequency band.

(a)

(b)

Figure 4.6 simulated results of the proposed antenna. (a) Reflection coefficient, (b) Gain

Figure 4-3(a-d) shows simulated radiation patterns of the antenna at some frequencies within the operational band in the xz and yz -planes respectively. The frequencies were chosen to represent the patterns in the low, mid and high frequency end of the operating bandwidth. The theta plots in red represent the co-pol components of the radiated waves whereas the phi plots in black represent the cross-pol components. It is observed that the proposed antenna has near stable radiation patterns across the operating bandwidth albeit with high cross pol patterns at some frequencies due to the asymmetrical nature of the antenna.



(a)

(b)



(d)

Figure 4.7 simulated radiation patterns of the proposed antenna at (a) 5 GHz, (b) 7 GHz (c) 9 GHz (d) 11 GHz

Due to unavailability of fabrication facilities in the country as well the unavailability of

measurement equipment like Vector network analyzers and facilities like an anechoic chamber, the designed antenna could not be fabricated and tested to validate the simulation results. However, HFSS which is the simulation tool that was used to design the proposed antenna has proven to be a very effective tool when it comes to the design of microwave devices like the slot antenna designed in this project.

Table 4.2 Results Compared to Other Results in the Literature

Reference antenna (year)	Antenna Size (mm ²)	Impedance Bandwidth
He et al (2021)	150 * 150	1.66-3.44 GHz (1.78 GHz)
Aiting et al (2021)	37 * 37	2.07 – 5.94 GHz (3.87 GHz)
Ritish et al (2018)	100 * 100	2.51 - 4.18 GHz (1.67 GHz)
Ellis et al (2016)	25 * 25	3.5 to 9.25 GHz (5.75 GHz)
Nakao et al (2010)	41 * 41	4.06 - 7.95 GHz (3.89 GHz)
Proposed Antenna	20 * 20	4.2 – 12.8 GHz (8.6 GHz)

The proposed antenna in this work is compared to some reference antennas in literature as shown in Table 4-2. It is observed that the proposed antenna offers a broader impedance bandwidth (8.6 GHz) than all the antennas in the Table as well as possessing a compact size. This shows that the proposed antenna has a competitive edge over the currently existing antennas in literature.

4.4 Link Budget Analysis

The link budget consists of the total budget of all elements in the telecommunication system between BTS and MS (and vice-versa). This includes antenna gains on both sides coaxial cabling between antenna and receiver/transmitter losses in duplexers,

splitters, connectors, gain of any amplifiers (PA, LNA) and the path loss of the radio link between the two antennas. A link budget analysis is undertaken in this section to show how effective the proposed antenna in this work will be for WLAN applications as compared to an isotropic antenna.

There are a number of models that can be utilized to undertake a link budget analysis including, the free space model, two ray model, log distance model, log normal model, etc. For the purpose of this work, the free space model is chosen as it provides a theoretically simpler frame than the other models albeit less accurate than the others.

The main parameters that are of interest in the analysis from this section are the received power and pathloss between the transmitter and receiver.

From the free space model, the received power is given by the equation:

$$P_r[d] \text{ (dB)} = 10 \log \left(\frac{P_t G_r G_t c^2}{(4\pi f_c d)^2} \right) \quad \text{equation 4.1}$$

Where, $P_r(d)$ = received power at distance d

P_t = transmit power

G_r = receiver gain

G_t = transmitter gain

c = speed of light

f_c = center frequency

d = distance between transmitter and receiver.

For the purpose of this work, the WLAN (WiFi) application at 5.8 GHz is chosen. One of the

advantages of the proposed antenna as already stated is its broad bandwidth which makes it suitable for the chosen application. WiFi is a low power application and as such, a transmit power of 1mW is chosen. The gain of the proposed antenna is 5dBi at a frequency of 5.8GHz as seen from the gain plots in the previous section and the performance is studied over a distance of 150 m. The analysis is compared to an isotropic antenna with a gain of 0 dB to show how effective the proposed antenna will be.

A Matlab program is written to implement equation 4.1 and the results are plotted in Figure 4.8 below. It is observed that a very considerable received power which is greater than -80 dB over the 150 m distance chosen for the analysis is realized when the proposed antenna is used. This is as a result of the 5dBi gain of the proposed antenna at the chosen center frequency. This goes to show that the antenna can work effectively as a WLAN antenna.

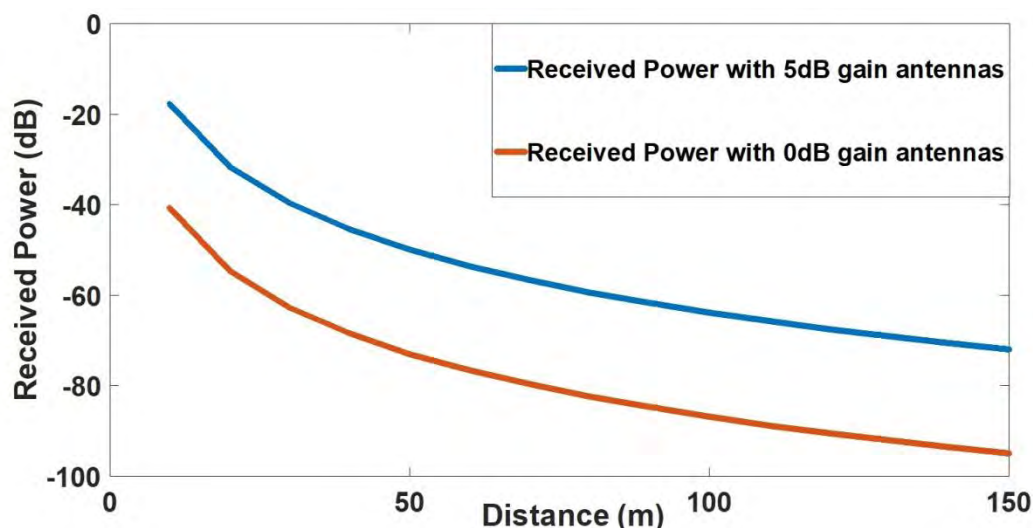


Fig 4.8. Received power over a varying Tx-Rx distances

A fundamental concept in planning any type of radio communications link is the concept of Path Loss. Path Loss describes the amount of signal loss (attenuation) between a receiver and a transmitter. It can also be described as the reduction in power density (attenuation) of an electromagnetic wave as it propagates through space. Path loss is a major component in the analysis and design of the link budget of a telecommunication system as already stated. Using the free space model, the path loss is given by:

$$PL (dB) = 10 \log \left(\frac{4\pi d f_c}{c} \right)^2 \quad \text{equation 2}$$

Where the variables have the same definitions as that of equation 4.1. A Matlab code is written to implement equation 4.2 and the results are depicted in Figure 4.9.

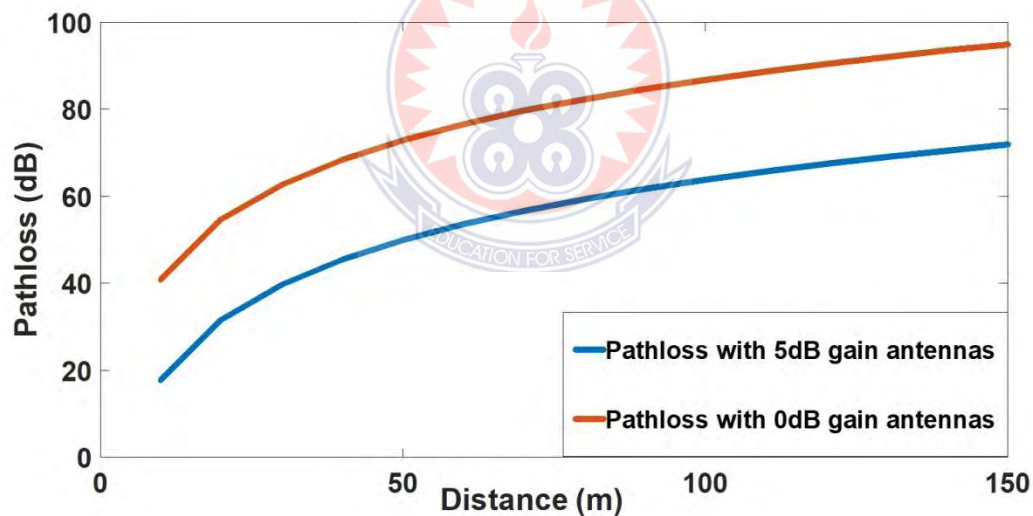


Fig 4.9. Pathloss over varying Tx-Rx distances

It is observed from Figure 4.9 that the path loss is less than 75 dB over the entire 150 m chosen for the analysis, which goes to confirm the results achieved from Figure 4.8. It can also be seen from both Figures 4.8 and 4.9 that the proposed antenna is more effective for WLAN applications as compared with the isotropic antenna which has a

gain of 0 dB.

The matlab codes that were used have been reproduced in the Appendix.



CHAPTER FIVE

SUMMARY OF FINDINGS, CONCLUSION AND RECOMMENDATIONS

This chapter presents a summary of the findings, makes a general conclusion to the study and recommends measures to address some of the inherent challenges identified in the study. This study sought to design a compact broadband planar slot antenna, to apply the developed antenna to future communication network such as 5G networks and beyond, and to simulate the developed broadband planar slot antenna to measure its efficiency.

5.1 Summary of Findings

Design of the Antenna

The proposed antenna had the basic configuration of a microstrip slot antenna. The design of the antenna chooses the center frequency as $f_c = 8$ GHz ($\lambda = 37.5$ mm, where, λ is the wavelength at 8 GHz). The wavelength is calculated by using the formula and half of the value obtained ($37.5/2$ mm) is used as the starting dimension of the designed antenna which is then optimized in the simulation tool to arrive at the dimension.

The designed antenna is composed of an L-shaped slot etched in the ground plane made of copper, a stub attached to the ground plane with a rectangular slot as well to aid in effective coupling between the feedline which is etched on the opposite side of the ground plane on the same dielectric substrate and the radiating L-slot. The

feedline has a slot etched in its midpoint and has a stub attached to it.

The ground plane with the slot and microstrip feedline are all etched on an FR4-epoxy dielectric substrate with a thickness of $h = 1.6\text{mm}$ and relative permittivity (ϵ_r) of 4.4.

The antenna has a ground plane size of G . The radiating L slot is designed by first subtracting the vertical side with dimensions ($L_s * e$) from the copper on the ground plane and then subtracting the horizontal portion with dimension ($W_s * h$) as well. A slot with a size of ($b * g$) is etched in the lower side of the ground plane

Simulation Performance

The simulation was done using the commercially available Ansoft HFSS 19 simulation tool which is based on FEM. The simulated reflection coefficient was found to be less than -10dB over the frequency ranges of $4.2 - 12.8\text{ GHz}$ which covers the entire IEEE C-Band and X-Band. This was linked to the effective coupling of the EM waves from the feedline to the wide slot which was made possible by the slot shape and stubs attached to both the feedline and the ground plane. The antenna was found with a gain above 2.5dB in almost the entire operating frequency band.

It was also observed that the proposed antenna has near stable radiation patterns across the operating bandwidth albeit with high cross pol patterns at some frequencies due to the asymmetrical nature of the antenna.

The antenna however could not be fabricated to validate the simulation results. This

was due to unavailability of fabrication facilities in the country as well the unavailability of measurement equipment like Vector network analyzers and facilities like an anechoic chamber, the designed antenna could not be fabricated and tested to validate the simulation results.

Link Budget Analysis

The analysis was compared to an isotropic antenna with a gain of 0 dB to show how effective the proposed antenna will be. It was observed that a very considerable received power which is greater than -80 dB over the 150 m distance chosen for the analysis is realized when the proposed antenna is used. This is as a result of the 5dBi gain of the proposed antenna at the chosen center frequency. The results suggested that the antenna can work effectively as a WLAN antenna. It was further observed that the path loss is less than 75 dB over the entire 150 m chosen for the analysis.

5.2 Conclusion

The proposed antenna in this study is the broadband planar slot antenna. It is a compact multiband resonance antenna with very good impedance bandwidth and return loss. Consequently, the conception and the simulation of a new low cost rectangular planar antenna is performed based on the theoretical equations to find out the initial antenna dimensions. Several findings were made and discussed. A key finding of the study is that the proposed antenna has near stable radiation patterns across the operating bandwidth albeit with high cross pol patterns at some frequencies

due to the asymmetrical nature of the antenna.

The increase in the development of broadband wireless access technologies for evolving wireless, mobile internet service and next generation cellular systems have been significant. The key advantages of a slot antenna are its small size, simple design, and ease of mass manufacture using waveguide or PC board technology. It is important therefore that local capacity is developed to explore the production of these antennas locally to meet the growing interest in the product.

5.3 Recommendations

This work can be further improved by implementing the antenna as a circular polarized antenna to solve the issues of polarization.



It is recommended that future work focuses on developing techniques to reduce the cross pol levels in the radiation pattern especially in the high frequency range

Also, techniques to make the antenna reconfigurable should be explored to avoid the need for extra signal processing circuits to switch between frequencies when the antenna is deployed in a device.

REFERENCES

- Aiting Wu , Furan Zhu , Pengquan Zhang , Zhonghai Zhang , and Boran Guan, Bandwidth Enhancement of a Microstrip-Line-Fed Printed Rotated Wide-Slot Antenna Based on Self-Shape Blending Algorithm, *Hindawi International Journal of Antennas and Propagation* Volume 2021, Article ID 9913822, pp. 10-14 <https://doi.org/10.1155/2021/9913822>
- Akhavan, H. G., & Mirshekar-Syahkal, D. (1994). Approximate model for microstrip fed slot antennas. *Electronics Letters*, 30(23), 1902-1903.
- Axelrod, A., Kisliuk, M., & Maoz, J. (1989). Broadband microstrip-fed slot radiator. *Microwave Journal*, 32, 81.
- Booker, H. G. (1946). Slot aerials and their relation to complementary wire aerials (Babinet's principle). *Journal of the Institution of Electrical Engineers-Part IIIA: Radiolocation*, 93(4), 620-626.
- Burns, R (2000). The life and times of A.D. Blumlein. Institution of Engineering and Technology. ISBN 0-85296-773-X.
- Chen, T. L., & Lin, Y. D. (1998). Aperture-coupled microstrip line leaky wave antenna with broadside mainbeam. *Electronics Letters*, 34(14), 1366-1366.
- Chen, W. S., Wu, C. K., & Wong, K. L. (2001). Novel compact circularly polarized square microstrip antenna. *IEEE Transactions on Antennas and Propagation*, 49(3), 340-342.
- Chen, W. S., Wu, C. K., & Wong, K. L. (1998). Compact circularly polarised microstrip antenna with bent slots. *Electronics Letters*, 34(13), 1278-1279.
- Chiu, C. Y., Li, J., Song, S., & Murch, R. D. (2012). Frequency-reconfigurable pixel slot antenna. *IEEE Transactions on Antennas and Propagation*, 60(10), 4921-4924.
- Ciais, P., Staraj, R., Kossiavas, G., Luxey, C. (2004), Design of an Internal Quad-Band

- Antenna for Mobile Phones, *IEEE Microwave and Wireless Components Letters*, vol. 14, no 4, p. 148-150, April. 2004.
- Constantine A. Balanis (2016), "Antenna Theory Analysis and Design 4th Ed.," John Wiley and sons, Hoboken, New Jersey.
- Covington, Arthur E. (1991). "Some recollections of the radio and electrical engineering division of the National Research Council of Canada, 1946-1977". *Scientia Canadensis: Canadian Journal of the History of Science, Technology and Medicine*. **15** (2): 155–175. doi:10.7202/800334ar.
- Deal, W. R., Qian, Y., Itoh, T., & Radisic, V. (1999). Planar integrated antenna technology. *Microwave Journal*, *42*(7), 128-137.
- Deng, J. Y., Yin, Y. Z., Huang, Y. H., Ma, J., & Liu, Q. Z. (2009). Compact circularly polarized microstrip antenna with wide beamwidth for compass satellite service. *Progress In Electromagnetics Research Letters*, *11*, 113-118.
- Deng, S. M., M. D. Wu, and P. Hsu, (1995) "Analysis of coplanar waveguide-fed microstrip antennas," *IEEE Trans. Antennas and Propagation*, Vol. 43, 734–737, July 1995.
- Ellis, M. S., Zhao, Z., Wu, J., Ding, X., Nie, Z., & Liu, Q. H. (2016). A novel simple and compact microstrip-fed circularly polarized wide slot antenna with wide axial ratio bandwidth for C-band applications. *IEEE Transactions on Antennas and Propagation*, *64*(4), 1552-1555.
- Ellis, M. S. (2013). Miniature staircase profile printed monopole antenna for ultrawideband applications. In *2013 Cross Strait Quad-Regional Radio Science and Wireless Technology Conference* (pp. 237-240). IEEE.
- Fan, S. T., Yin, Y. Z., Lee, B., Hu, W., & Yang, X. (2012). Bandwidth enhancement of a printed slot antenna with a pair of parasitic patches. *IEEE antennas and*

wireless propagation letters, 11, 1230-1233.

Garg, R., Bhartia, P., Bahl, I. J., & Ittipiboon, A. (2001). *Microstrip antenna design handbook*. Artech house.

Gauthier, G. P., Courtay, A., & Rebeiz, G. M. (1997). Microstrip antennas on synthesized low dielectric-constant substrates. *IEEE Transactions on Antennas and Propagation*, 45(8), 1310-1314.

Gayathri, C., & Kavitha, V. (2015). Mitigation of Colluding Selective Forwarding Attack in WMN's using FADE. *International Journal for Trends in Engineering and Technology*, 3(1), 6-12.

He W, He Y, Wong S-W, Liao C-H. (2021), "A wideband circularly polarized S-shaped slot antenna", *Int J RF Microw Comput Aided Eng.*, 2021.

Himdi, M., & Daniel, J. P. (1992). Analysis of printed linear slot antenna using lossy transmission line model. *Electronics letters*, 28(6), 598-601.

Ito, K., Aizawa, N., & Goto, N. (1979). Circularly polarised printed array antennas composed of strips and slots. *Electronics Letters*, 15(25), 811-812.

Jan, J. Y., & Su, J. W. (2005). Bandwidth enhancement of a printed wide-slot antenna with a rotated slot. *IEEE transactions on antennas and propagation*, 53(6), 2111-2114.

Jan, J. Y., & Wang, L. C. (2009). Printed wideband rhombus slot antenna with a pair of parasitic strips for multiband applications. *IEEE Transactions on antennas and propagation*, 57(4), 1267-1270.

Jen-Yea, J., Liang-Chin, W. (2009). Printed wideband rhombus slot antenna with a pair of parasitic strips for multiband applications. *IEEE Trans Antennas Propagat.*

Kahrizi, M., Sarkar, T. K., & Maricevic, Z. A. (1993). Analysis of a wide radiating slot in the ground plane of a microstrip line. *IEEE Transactions on Microwave Theory and Techniques*, 41(1), 29-37.

- Kavitha, V., &Palanisamy, V. (2013). New burst assembly and scheduling technique for optical burst switching networks. *Journal of Computer Science*, 9(8), 1030.
- Kavitha, V., &Gayathri, C. (2015).an Analysis on Routing and Issues in Network Layer in WMN's. *International Journal of Scientific and Engineering Research*, 6(4), 120-125.
- Kavitha, V., &Vidya, S. V. (2015). A grid based vehicle localization system providing safety precautions. *International Journal of Applied Engineering Research*, 10(1), 940-944.
- Kamal, B., Ahmed, M., Abdelkader, Y. (2017) A Novel Planar Slot Antenna Structure for 5G Mobile Networks Applications. *Journal of Electrical and Electronic Engineering*. Vol. 5, No. 4, 2017, pp. 111-115. doi: 10.11648/j.jeee.20170504.11
- Kerketta, J., &Behera, S. R. (2012). *Design of Fractal slot Antennas for WLAN and WiMAX Applications* (Doctoral dissertation).
- Kim, J. P., & Park, W. S. (1998).Network modeling of an inclined and off-center microstrip-fed slot antenna. *IEEE Transactions on Antennas and Propagation*, 46(8), 1182-1188.
- Lin, Y. D., Sheen, J. W., &Tzuang, C. K. (1996). Analysis and design of feeding structures for microstrip leaky wave antenna. *IEEE transactions on microwave theory and techniques*, 44(9), 1540-1547.
- Lin, Y. D., & Sheen, J. W. (1997).Mode distinction and radiation-efficiency analysis of planar leaky-wave line source. *IEEE Transactions on Microwave Theory and Techniques*, 45(10), 1672-1680.
- Mahmoud, M. N., &Baktur, R. (2011).A dual band microstrip-fed slot antenna. *IEEE Transactions on antennas and propagation*, 59(5), 1720-1724.
- Nakao, S., Joseph, R., &Fukusako, T. (2010). A circularly polarized L-shaped and rectangular slot antenna with an L-shaped probe for wideband characteristics. In *2010 Asia-Pacific Microwave Conference* (pp. 734-737).IEEE.

- PalanivelRajan, S. (2015). Review and investigations on future research directions of mobile based telecare system for cardiac surveillance. *Journal of applied research and technology*, 13(4), 454-460.
- Qian, Y., Coccioli, R., Sievenpiper, D., Radisic, V., Yablonovitch, E., &Itoh, T. (1999). A microstrip patch antenna using novel photonic band-gap structures. *Microwave Journal*, 42(1), 66-72.
- Qian, Y., &Itoh, T. (1997, December).A broadband uniplanar microstrip-to-CPS transition. In *Proceedings of 1997 Asia-Pacific Microwave Conference* (pp. 609-612). IEEE.
- Qian, Y., Chang, B. C. C., Itoh, T., Chen, K. C., &Tzuang, C. K. C. (1999, June).High efficiency and broadband excitation of leaky mode in microstrip structures. In *1999 IEEE MTT-S International Microwave Symposium Digest (Cat. No. 99CH36282)* (Vol. 4, pp. 1419-1422).IEEE.
- Pozar, D. M. (1992).Microstrip antennas. *Proceedings of the IEEE*, 80(1), 79-91.
- Pozar, D. A. V. I. D. M. (1986). A reciprocity method of analysis for printed slot and slot-coupled microstrip antennas. *IEEE Transactions on Antennas and Propagation*, 34(12), 1439-1446.
- Rajan, S. P., Sukanesh, R., Kamalesswaren, T., Prasaanth, R., &Thangaperumal, P. (2012).Performance analysis of mobile phone radiation minimization through characteristic impedance measurement. *International Journal of Computer Science Issues (IJCSI)*, 9(2), 540.
- Radisic, V., Qian, Y., &Itoh, T. (1998).Novel architectures for high-efficiency amplifiers for wireless applications. *IEEE Transactions on Microwave Theory and Techniques*, 46(11), 1901-1909.
- Rajan, S. P. (2014). A Significant and Vital Glance at “Stress and Fitness Monitoring Embedded on a Modern Telematics Platform”. *Telemedicine and e-Health*, 20(8), 757-758.

- Rebeiz, G. M. (1992). Millimeter-wave and terahertz integrated circuit antennas. *Proceedings of the IEEE*, 80(11), 1748-1770.
- Ritish, K., Piyush, S., and Praveen Kumar, A V. (2018). "Offset fed slot antenna for broadband operation", IOP Conf. Series: Materials Science and Engineering 331 012022 doi:10.1088/1757-899X/331/1/012022
- Roh W. et al. (2014), "Millimeter-Wave Beamforming as an enabling technology for 5G cellular communications: theoretical feasibility and prototype results", *IEEE Comm. Magazine*, pp. 106-113, Feb. 2014.
- Roy, J., & Themalil, M. T. (2008). Design of a circularly polarized microstrip antenna for WLAN. *Progress In Electromagnetics Research M*, 3, 79-90.
- Run-Nan, C., Ming-Chuan, Y., Shu, L., Xing-Qi, Z., Xin-Yue, Z., & Xiao-Feng, L. (2012). Design and analysis of printed Yagi-Uda antenna and two-element array for WLAN applications. *International journal of antennas and propagation*, 2012.
- Saed, M., (2005) "Reconfigurable broadband microstrip antenna fed by a coplanar waveguide," *Progress In Electromagnetics Research*, PIER 55, 227–239, 2005.
- Sasikumar, P., Vivek, C., & Jayakrishnan, P. (2010). Key-management systems in vehicular ad-hoc networks. *International Journal of Computer Applications*, 10(1), 23-28.
- Scholz, D. I. P., & Kathrein-Werke, K. G. (2000). Basic antenna principles for mobile communications. *Polarization*, 45(45), 12.
- Sharma, A., Das, G., Gupta, S., & Gangwar, R. K. (2020). Quad-band quad-sense circularly polarized dielectric resonator antenna for GPS/CNSS/WLAN/WiMAX applications. *IEEE Antennas and Wireless Propagation Letters*, 19(3), 403-407.
- Shin, Y. S., Park, S. O., & Lee, M. (2005). A broadband interior antenna of planar monopole type in handsets. *IEEE Antennas and wireless propagation letters*, 4, 9-12.

- Srinivasan, M., & Annadurai, S. (2017, April). A bandwidth analysis using broadband dual-polarization and stable-beam width slot antenna fed by U-shape micro strip line. In *2017 IEEE International Conference on Electrical, Instrumentation and Communication Engineering (ICEICE)* (pp. 1-4). IEEE.
- Srinivasan, M., & Annadurai, S. (2017, April). A bandwidth analysis using broadband dual-polarization and stable-beam width slot antenna fed by U-shape micro strip line. In *2017 IEEE International Conference on Electrical, Instrumentation and Communication Engineering (ICEICE)* (pp. 1-4). IEEE.
- Sukanesh, R., Gautham, P., Arunmozhivarman, P. T., & Vijayprasath, S. (2010, October). Cellular phone based biomedical system for health care. In *2010 International Conference On Communication Control And Computing Technologies* (pp. 550-553). IEEE.
- Sundaravadivu, K., & Bharathi, S. (2013, March). STBC codes for generalized spatial modulation in MIMO systems. In *2013 IEEE International Conference ON Emerging Trends in Computing, Communication and Nanotechnology (ICECCN)* (pp. 486-490). IEEE.
- Tsai, H. S., Rodwell, M. J. W., & York, R. A. (1994). Planar amplifier array with improved bandwidth using folded-slots. *IEEE Microwave and Guided wave letters*, 4(4), 112-114.
- Xu, L., Li, L., & Zhang, W. (2014). Study and design of broadband bow-tie slot antenna fed with asymmetric CPW. *IEEE Transactions on Antennas and Propagation*, 63(2), 760-765.
- Vasudevan, S. K., Vivek, C., & Srivathsan, S. (2015). An intelligent boxing application through augmented reality for two users—human computer interaction attempt. *Indian Journal of Science and Technology*, 8(34), 1-7.
- Visser, H. I. (2013). *Multiband microstrip slot antenna with multiple-input and multiple-output (MIMO) implementation for handheld devices* (Doctoral dissertation, San Diego State University).

- Wang, Y., & Du, Z. (2015). Dual-polarized slot-coupled microstrip antenna array with stable active element pattern. *IEEE Transactions on Antennas and Propagation*, 63(9), 4239-4244.
- Weller, T. M., Katehi, L. P., & Rebeiz, G. M. (1995). Single and double folded-slot antennas on semi-infinite substrates. *IEEE Transactions on antennas and propagation*, 43(12), 1423-1428.
- Wu, J. G., & Zhou, X. M. (2012, May). A design of miniaturization dual-frequency antenna for GPS and WLAN application. In *2012 International Conference on Microwave and Millimeter Wave Technology (ICMMT)* (Vol. 4, pp. 1-3). IEEE.
- Yang, S., Lee, K. F., Kishk, A., & Luk, K. M. (2008). Design and study of wideband single feed circularly polarized microstrip antennas. *Progress In Electromagnetics Research*, 80, 45-61.
- Yi Huang, Y., and Boyle, K. (2008), "Antennas From Theory To Practice", John Wiley and sons.
- Yoshimura, Y. (1972). A microstripline slot antenna (short papers). *IEEE Transactions on Microwave Theory and Techniques*, 20(11), 760-762.
- Zaker, R., & Abdipour, A. (2011). Dual-wideband circularly-polarised slot antenna using folded L-shaped stub. *Electronics Letters*, 47(6), 361-363.
- Zhang, X. Q., Jiao, Y. C., & Wang, W. H. (2012). Compact wide tri-band slot antenna for WLAN/WiMAX applications. *Electronics Letters*, 48(2), 64-65.
- Zhang, Li, Y. Jiao, Yang Ding, Bo Chen, and Z. Weng. (2013). CPW-fed broadband circularly polarized planar monopole antenna with improved ground-plane structure. *IEEE Transactions On Antennas And Propag.*, Vol. 61, 4824-4828, Sep.2013. doi:10.1109/TAP.2013.2267719

APPENDIX

Matlab code for received power calculation:

```

%clear workspace and all plots
close all
clear
clc

%distance ranges
d = 10:10:150;

% %reference distance
% d1 = 10;

%speed of signal in vacuum
c = 3*10e8;

%frequency
f = 5.8e6;

Gt_db = 5; % gain for both receive antenna
Gr_db = 5; % gain for transmit antenna

% to change from dB;
Gt = 10^(Gt_db/10);
Gr = 10^(Gr_db/10);
Pt = 1e-3;

%received power using the Free Space PathLoss model at different distances
Received_power_at_5db = 10*log((Pt*Gt*Gr*c.^2)/((4*pi*f*d).^2));

Received_power_at_0db = 10*log((Pt*1*1*c.^2)/((4*pi*f*d).^2));

plot(d,Received_power_at_5db,d,Received_power_at_0db)
xlabel('Distance (m)')
ylabel('Received Power (dB)')
legend('Received Power with 5dB gain antennas','Received Power with 0dB gain antennas')

```

Matlab Code for Pathloss calculation:

```

%clear workspace and all plots
close all
clear
clc

%distance ranges

```

```

d = 10:10:150;

%speed of signal in vacuum
c = 3*10e8;

%frequency
f = 5.8e6;

Gt_db = 5; % gain for both transmit antenna
Gr_db = 5; % gain for receiver antenna

% to change from dB;
Gt = (10^(Gt_db/10))*0.001;
Gr = (10^(Gr_db/10))*0.001;
Pt = 1e-3;

%Pathloss using the Free Space PathLoss model at different distances
Pathloss_at_5db = -10*log((Pt*Gt*Gr*c.^2)/((4*pi*f*d).^2));

Pathloss_at_0db = -10*log((Pt*1*1*c.^2)/((4*pi*f*d).^2));

plot(d,Pathloss_at_5db,d,Pathloss_at_0db)
xlabel('Distance (m)')
ylabel('Pathloss (dB)')
legend('Pathloss with 5dB gain antennas','Pathloss with 0dB gain antennas')

```

